Stimulus-to-stimulus learning in RNNs with cortical inductive biases

Pantelis Vafidis[1*] and Antonio Rangel[2]

[1]Computation & Neural Systems, California Institute of Technology, Pasadena, CA 91125
[2]Humanities and Social Sciences, California Institute of Technology, Pasadena, CA 91125
[*]pvafeidi@caltech.edu

September 23, 2024

Summary

Animals learn to predict external contingencies from experience through a process of conditioning. A natural mechanism for conditioning is stimulus substitution, whereby the neuronal response to a stimulus with no prior behavioral significance becomes increasingly identical to that generated by a behaviorally significant stimulus it reliably predicts. We propose a recurrent neural network model of stimulus substitution which leverages two forms of inductive bias pervasive in the cortex: representational inductive bias in the form of mixed stimulus representations, and architectural inductive bias in the form of two-compartment pyramidal neurons that have been shown to serve as a fundamental unit of cortical associative learning. The properties of these neurons allow for a biologically plausible learning rule that implements stimulus substitution, utilizing only information available locally at the synapses. We show that the model generates a wide array of conditioning phenomena, and can learn large numbers of associations with an amount of training commensurate with animal experiments, without relying on parameter fine-tuning for each individual experimental task. In contrast, we show that commonly used Hebbian rules fail to learn generic stimulus-stimulus associations with mixed selectivity, and require task-specific parameter fine-tuning. Our framework highlights the importance of multi-compartment neuronal processing in the cortex, and showcases how it might confer cortical animals the evolutionary edge.

Keywords. Associative learning, classical conditioning, recurrent neural networks, synaptic plasticity, predictive coding, stimulus substitution, mixed selectivity, compartmentalized neuron, self-supervised learning, surprise.

Introduction

The ability to forecast important events is necessary for effective behavior. Animals are equipped with innate reflexes to tackle common threats and to exploit opportunities in their environment. However, given the complex and changing nature of the world, animals also need to acquire new reflexes by learning from experience. This process involves the association or conditioning of an initially neutral stimulus (conditioned stimulus, CS) with another stimulus intrinsically related to primary reward or punishment (unconditioned stimulus, US). If learning is successful, the CS can then induce the same behavioral response as the US. Initially proposed by Pavlov, this type of learning is known as classical conditioning.

A potential mechanism for conditioning is stimulus substitution [1]. Under this mechanism, the response of the relevant population of neurons to the CS becomes increasingly identical to that generated by the US. After this, any downstream processes that are normally triggered by the US are also triggered by the CS. Behavioral evidence in favor of stimulus substitution comes from studies showing that animals display the same behavior to the CS as to the US, even when the behavior is not appropriate (e.g. consummatory response towards a light that has been associated with food), and that the behavior is reinforcer dependent [1]. Furthermore, recent experiments show that during conditioning the response of S1 pyramidal neurons to the CS becomes increasingly similar to their response to the US, a phenomenon the authors termed "learning induced neuronal identity switch", and that this change correlates with learning performance [2].

A basic goal in computational and cognitive neuroscience is to build plausible models of neural network architectures capable of accounting for psychological phenomena. Previous work has shown that three-factor Hebbian synaptic plasticity rules accounts for a wide gamut of conditioning phenomena [3–6]. However, these models have some important limitations. First, they fail to capture the generality of pattern-to-pattern associations implicit in stimulus substitution, where both the US and the CS correspond to population activity patterns. Some use learning rules requiring storage of recent events at each synapse [5], while most assume that the tuning of neurons to stimuli is demixed, allowing simple reward modulated spike-timing-dependent plasticity to establish the appropriate mappings [5, 6]. These assumptions are inconsistent with the well-established fact that representations throughout the brain are high-dimensional and mixed [7].

In this study we propose a recurrent neural network (RNN) model of stimulus substitution. Critically, the model learns pattern-to-pattern associations using only biologically plausible local plasticity, and individual neurons are tuned to multiple behavioral stimuli, which gives rise to mixed representations of the CSs and USs. While subcortical [8] and even single-neuron [9] mechanisms for conditioning exist, our model is focused on stimulus-stimulus learning in the cortex, where the use of mixed stimulus representation allows learning a wide and flexible range of associations within the same neuronal network, which confers an evolutionary edge.

To achieve this goal, we leverage two forms of biological inductive bias built into the cortex: first, representational inductive bias in the form of mixed stimulus representations, that permit the efficient packing of multiple associations within the same neuronal population. To combat the additional complexity introduced by mixed representations, which requires not just the activation of the correct neurons but also the correct activity level, we leverage the second form of inductive

bias: architectural inductive bias in the form of two-compartment layer-5 pyramidal neurons which are prevalent in the cortex [10].

We propose a *RNN* model of such two-compartment neurons. Recent work has shown that these neurons can learn to be predictive of a reward [11], and suggests that they could serve as a fundamental unit of associative learning in the cortex through a built-in cellular mechanism [12]. Hence, we refer to them as associative neurons. The term associative here does not have a strictly Hebbian interpretation; rather it refers to the *hetero*-associative capacity of these neurons to link together information originating from different streams [13], through a mechanism known as BAC firing [14]. The properties of these neurons allow for a biologically plausible learning rule that utilizes only information available locally at the synapses, and that is capable of inducing self-supervised predictive plasticity [15, 16], which allows neurons to respond with the same firing rate to the *CS* as they would to the *US*, i.e. achieve stimulus substitution.

We show that the model generates a wide array of conditioning phenomena, including delay conditioning, trace conditioning, extinction, blocking, overshadowing, saliency effects, overexpectation, contingency effects and faster reacquisition of previous learnt associations. Furthermore, it can learn large numbers of *CS-US* associations with an amount of training commensurate with animal experiments, without relying on parameter fine-tuning for each individual experimental task. In contrast, we show that Hebbian learning rules, including three-factor extensions of Oja's rule [17] and the BCM rule [18], fail to learn generic stimulus-to-stimulus associations due to their unsupervised nature, and require task specific parameter fine-tuning.

Results

Model setup

In classical conditioning animals learn to predict the upcoming appearance of an unconditioned stimulus (*US*, e.g. food) after the presentation of a conditioned stimulus (*CS*, e.g. bell ring). As shown in fig. 1A, trials start with the presentation of the *CS*, which lasts until $t_{\text{cs-off}}$. The *US* is presented at $t_{\text{us-on}}$, and lasts until the end of the trial. Each trial has a fixed duration of t_{trial} seconds. If the *US* appears before the *CS* disappears, the task involves delay conditioning. In contrast, if the *CS* disappears before the *US* is shown, the task involves trace conditioning, with $t_{\text{delay}} = t_{\text{us-on}} - t_{\text{cs-off}}$ denoting the delay between the two stimuli. In our task animals need to learn N_{stim} different *CS-US* pairs. Every trial one pair is randomly chosen, and the corresponding *CS* is shown followed by its associated *US*.

We model a *RNN* of associative neurons (fig. 1C, yellow background) that represents the stimuli using mixed population representations and is capable of learning all of the *CS-US* associations using only local information available at the synapses. The inputs to the model are time-dependent vectors $r_{\text{cs}}(t)$ and $r_{\text{us}}(t)$, of dimension N_{inp}, that encode the presence and identity of the *CS* and the *US*. For simplicity, these vectors are represented by unique Boolean vectors, and they take the value of the stimulus while it is shown, and zero otherwise. The vectors are randomly generated, subject to a constraint for a minimal Hamming distance H_{d} between any two vectors of the same type. This minimal separation limits the extent to which learning on any give pair impairs learning of the other associations. The output of the associative network
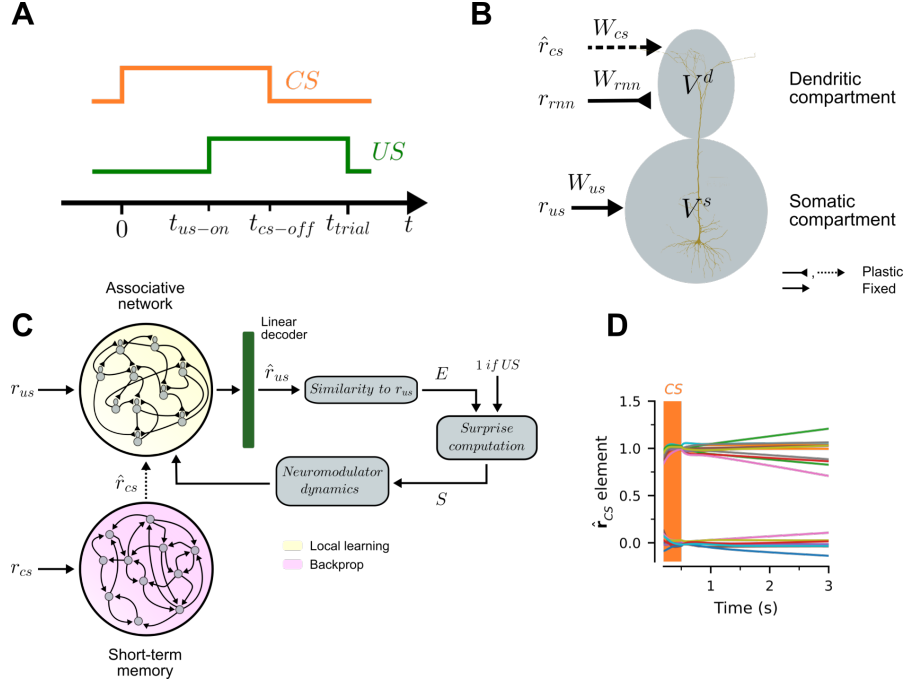
Figure 1: **Model**. (A) Every trial has a duration of t_{trial} seconds. Trials start with the presentation of a *CS*, which disappears after time $t_{\text{cs-off}}$. The associated *US* appears at time $t_{\text{us-on}}$ and stays until the end of the trial. The network has to learn N_{stim} unique *CS-US* pairs. (B) Associative neurons are modeled as an abstraction of a layer-5 cortical pyramidal neuron. V^{s} and V^{d} denote the voltage in the somatic and dendritic compartments. The somatic compartment receives as input a Boolean vector r_{us} representing the *US*. The dendritic compartment receives as inputs a vector $\hat{r}_{\text{cs}}$ with a short-term memory representation of the *CS*, as well as recursive activity from all other neurons in the *RNN*. The matrices W_{rnn}, W_{cs} and W_{us} denote the synaptic weights for the inputs. W_{us} is fixed throughout the experiment. W_{rnn} and W_{cs} are updated over trials with training. (C) Full outline of the model. The associative network is made of N_{rnn} associative neurons. The *US* is presented directly to the associative neurons, whereas the *CS* is presented to a short-term memory circuit that produces the short-term memory representation $\hat{r}_{\text{cs}}$. Learning in the associated network is gated by a surprise signal which measures the extent to which the *US*, or its absence, was anticipated. The surprise signal is computed in three steps. First, throughout the trial a linear decoder is used to obtain an estimate $\hat{r}_{\text{us}}$ of the *US* from the population vector of the associative network, denoted by r_{rnn}. Second, an expectation E^i is formed according for each *US* based on the similarity between r^i_{us} and $\hat{r}_{\text{us}}$. These expectations determine the level of surprise S associated with the arrival or absence of the *US*, which then gives rise to neuromodulator dynamics that gate learning in the associative network. (D) Performance of the short-term memory network in a single trial when *CS*s are presented only for 500 ms. We plot the output of the memory network for several seconds. Each color denotes a different element in r_{cs}.

is an estimate of the *US* vector r_{us}, denoted $\hat{r}_{\text{us}}$, which is decoded from network activity at all times (see fig. 1C and "*US* decoding" in Methods).

The fundamental unit of computation in the associative network is the associative neuron, a two-compartment neuron modelled after layer-5 pyramidal cells in the cortex (fig. 1B). A crucial property of the associative neuron is that it can separate incoming "feedforward" inputs from "feedback" ones, and compare the two to drive learning. In our case, since we are modelling a primary reinforcer cortical area, *US* inputs are assumed feedforward and arrive at the somatic

compartment (corresponding to the soma and proximal dendrites) through synaptic connections W_{us}, and *CS* inputs are considered feedback connections arriving to the distal dendrites from the rest of the cortex, along with local recurrent connections (W_{cs} and W_{rnn} respectively, fig. 1B). This separation of inputs ultimately allows for the construction of a biologically plausible predictive learning rule, capable of achieving stimulus substitution.

Specifically, to account for the ability of the associative neuron to predict its own spiking activity to somatic inputs from dendritic inputs alone [14], we utilize a synaptic plasticity rule that implements local error correction at the neuronal level [15]. The learning rule modifies the connections to the dendritic compartment (i.e. W_{cs} and W_{rnn}) in order to minimize the discrepancy between the firing rate of the neuron $f(V^{\text{s}})$ (where V^{s} is the somatic voltage, primarily controlled by *US* inputs in the beginning of learning, and f the activation function) and the prediction of the firing rate by the dendritic compartment $f(p'V^{\text{d}})$ (where V^{d} is the dendritic voltage, primarily controlled by *CS* inputs, and p' is a constant accounting for attenuation of V^{d} due to imperfect coupling with the somatic compartment). The synaptic weight $W_{\text{pre,post}}$ from a presynaptic neuron to a postsynaptic associative neuron is modified according to:

$$\Delta W_{\text{pre,post}} = \eta(S) \left[f(V^{\text{s}}_{\text{post}}) - f(p' V^{\text{d}}_{\text{post}}) \right] P_{\text{pre}} \tag{1}$$

where η is a variable learning rate which depends on a surprise signal S and P_{pre} the postsynaptic potential from the presynaptic neuron (for details, see "Synaptic plasticity rule" in Methods). In the Supplementary Information (section "Predictive coding and normative justification for the learning rule") we show how this learning rule can be derived directly from the objective of stimulus substitution.

During trace conditioning the *CS* disappears before the *US* appears, but an association is still learnt. This suggests that the brain maintains some short-term memory representation of the *CS* after it disappears. To capture this, we introduce a short-term memory *RNN* that maintains a (noisy) representation of the *CS*, denoted by $\hat{r}_{\text{cs}}$, over time (for details, see "*CS* short-term memory circuit" in Methods). As shown in fig. 1D, the network is able to maintain short-term representations of the *CS* for several seconds before memory leak becomes considerable.

Finally, the learning rule is gated by a surprise mechanism mediated by diffuse neuromodulator signals [19], as follows: Upon *CS* presentation, an expectation E is formed according to the proximity of $\hat{r}_{\text{us}}$ to r_{us} for known *US*s (see "*US* expectation estimation" in Methods). E can be thought of as the probability that some known *US* will appear. Upon *US* presentation, E is compared to 1 and a surpise signal $S = 1 - E$ is formed and gates learning; the greater the surprise, the greater the learning rate. If no *US* appears in the trial, then we set $S = -E$ at t_{wait} seconds after normal *US* presentation. Non-zero values of S activate learning, in a process driven by two neuromodulators, one for positive and another for negative learning rates (for details on dynamics, see "Surprise based learning rates" in Methods).

Network learns stimulus substitution in delay conditioning

Consider a delay conditioning experiment in which the animal needs to learn 16 *CS-US* pairs, and the timing of the trial is as shown in fig. 2A. Note that in this case the *CS* is present throughout the trial and, as a result, $\hat{r}_{\text{cs}} \approx r_{\text{cs}}$. Although the short-term memory network is not necessary in

this particular experiment, we keep it in the model to maintain consistency across experiments.

We train the *RNN* for a total of 1000 trials. Figure 2B compares the actual representations of all the *US*s, one component at a time, with those decoded from the activity of the network in response only to the associated *CS*s. The network has accurately learnt all of the associations after 500 training trials (≈ 32 per *CS-US* pair).
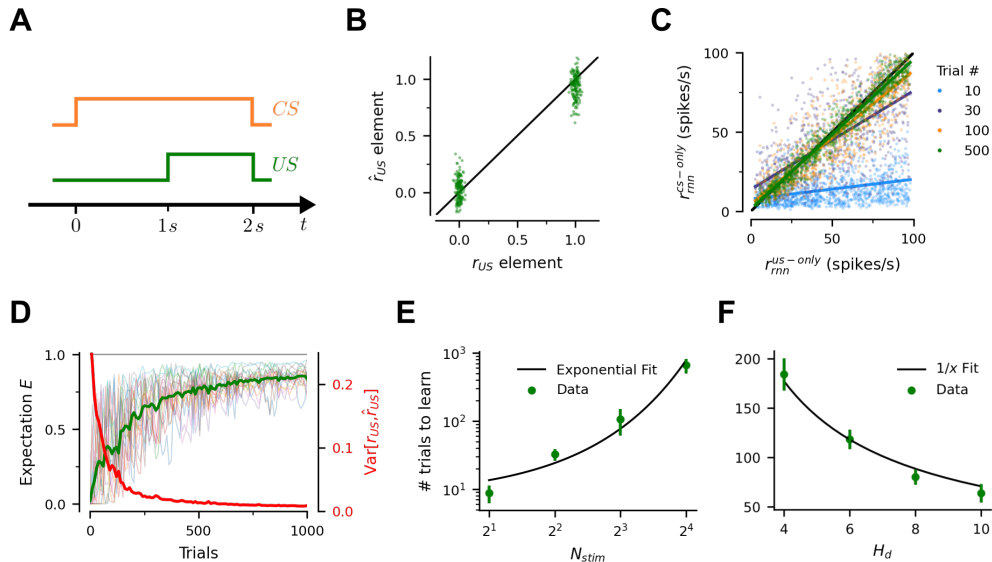
Figure 2: **Delay conditioning and stimulus substitution**. (A) Trial structure. The network is presented with $N_{\text{stim}} = 16$ different *CS-US* pairs, randomly selected in each trial. (B) The network learns all of the *CS-US* pairs after 500 training trials (≈ 32 per pair). r_{us} denotes the individual components of the Boolean vectors encoding each of the *US*s. $\hat{r}_{\text{us}}$ denotes the individual components of the decoded *US*s, based only on the presentation of the associated *CS*s, and measured just before the *US* appears. (C) Evolution of population responses during learning. Colors denote trial number. Each point compares the firing rate of an associate neuron at that stage of learning for a specific *CS-US* pair when only the *US*, or only the associated *CS* are presented. The colored lines are linear regression fits at each stage of learning. (D) Evolution of predicted *US* during learning. Green curve depicts the average expectation across *US*s after the network is presented only with the associated *CS*. Red curve depicts the distance between the true representation of the *US*s (r_{us}) and their decoded representation $\hat{r}_{\text{us}}$ when presented only with the associated *CS*. Individual pairs are shown in faint thin lines. (E) Number of trials required for the network to reach 80% performance for all pairs (defined as the first time at which the average expectation E across pairs exceeds 0.8) for different numbers of stimulus pairs. Performance is measured just before the *US* appears. Error bands denote $\mp$ SD computed across 5 different runs of the experiment. (F) Number of trials required to reach 80% performance for all pairs for different levels of similarity in the encoding of the *CS* and *US* input vectors. Error bands denote $\mp$ SD computed across 10 different runs of the experiment.

We next investigate how learning evolves with the amount of training. Figure 2C compares the activity of the associative neurons when presented only with the *US*, for all possible *CS-US* pairs, with their activity when presented only with the associated *CS*. Early in training, the associative neurons exhibit little activity in response to the *CS*s, and their responses are not correlated with the amount of activity elicited by the *US*s. By the end of training however, the neurons respond to the *CS* the same way they respond to the *US*, therefore stimulus substitution is achieved. A host of conditioning phenomena, detailed in following sections, follow from that.

For further details on the trial dynamics of learning see the Supplementary Information (section "How does the *RNN* learn?"). Importantly, in the Supplements we also show that three-factor Hebbian learning rules fail at stimulus substitution in our experiments.

Figure 2D tracks the learning dynamics more closely. The green curve shows the average expectation E assigned to the *US*s at different stages of training. Perfect learning occurs when $E = 1$ for all *US*s. The red curve provides a measure of distance between the r_{us} and $\hat{r}_{us}$. We see that learning requires few repetitions per *CS-US*, and is substantially faster early on.

There are three sources of randomness in the model: (1) randomness in the sampling of *CS* and *US* sets, (2) randomness in the order in which the stimulus pairs are presented, and (3) randomness in the initialization of W_{rnn}, W_{cs} and W_{us}. In fig. S5 we explore the impact of this noise in our results by training 5 networks with different initializations and training schedules. We find that the level of random variation across training runs is small, and is mostly dominated by randomness in the sampling of the stimuli. For this reason, unless otherwise stated, we present results using only a single training run.

Since the *RNN* uses mixed representations over the same neurons to encode the stimuli, one natural question is how does learning depend on the number of *CS-US* pairs in the experiment (N_{stim}) and on the similarity of their representations (r_{cs} vs r_{us}).

We explore the first question by training the model for different values of N_{stim} and then measuring the number of trials that it takes the network to reach a 80% level of maximum performance, defined as the level of training at which the average expectation E across pairs exceeds 0.8. Interestingly, the required number of trials increases exponentially with the number of *CS-US* pairs (fig. 2E). This is likely due to interference across pairs: learning of an association also results in unlearning of other associations at the single trial level. This interference gets worse as the number of stimuli N_{stim} increases (fig. S6), which might explain the exponential dependence. Finally, note that the network is capable of very fast learning when there are only a few pairs (about 5 presentations per pair for two pairs, fig. 2E).

We explore the second question by training the model for different values of the Hamming distances H_d, which provides a lower bound on the similarity among *US*s and, separately, among *CS*s. $N_{stim} = 8$ for these experiments. Perhaps unsurprisingly, the more dissimilar the stimulus representations, the faster the learning (fig. 2F). Figure S7 shows how smaller H_d naturally leads to greater interference across stimuli.

Short-term memory and trace conditioning

Next we consider trace conditioning experiments, in which there is a delay interval $t_{delay} > 0$ between the disappearance of the *CS* and the arrival of the *US* (fig. 3A). In this case the memory network is crucial for maintaining a memory trace of the *CS* to be associated with the *US*.

As before, we train the *RNN* for 1000 trials, with 16 different pairs, to explore how learning changes over time and how the delay $t_{delay} > 0$ affects learning. For comparison purposes, we include the case of delay conditioning in the same figures ($t_{delay} = -1$ s).

Figure 3B shows the quality of the decoded representation of the *US* and fig. 3C-D the strength of the associated expectation signal, both measured offline and in response only to the *CS*. We find that the *RNN* learns the associations well for small delays, but that the quality of the learning decays for larger delays. This pattern has been observed in animal experiments [20],
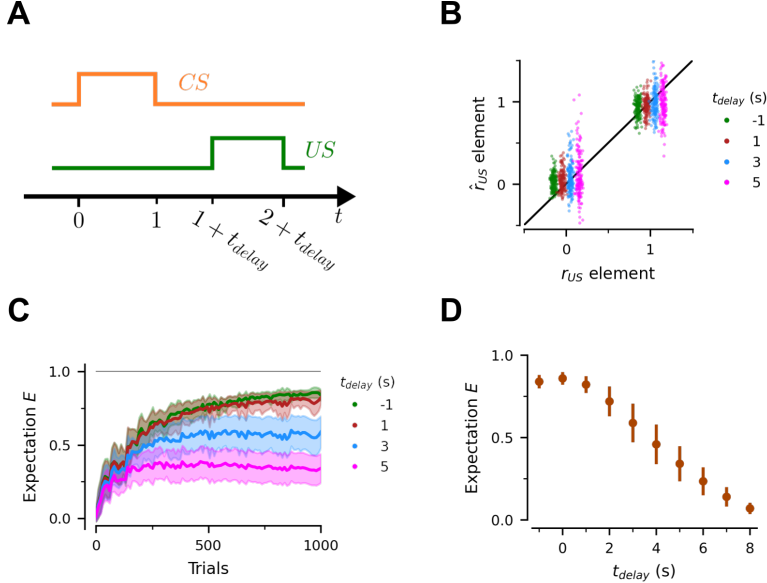
Figure 3: **Trace conditioning**. (A) Trial structure. The network is presented with $N_{\text{stim}} = 16$ different *CS-US* pairs, randomly selected in each trial. (B) After 500 training trials ($\sim$ 32 per pair), the network learns all of the *CS-US* pairs for short t_{delay}, but struggles for longer delays. r_{us} denotes the individual components of the Boolean vectors encoding each of the *US*s. $\hat{r}_{\text{us}}$ denotes the individual components of the decoded *US*s, based only on the presentation of the associated *CS*s. For comparison purposes, we also show results for delay conditioning ($t_{\text{delay}} = -1$) (C) Evolution of predicted *US* during learning. Each curve depicts the expectation for each *US* after the network is presented only with the associated *CS*. Line is the mean across all stimulus pairs. Bands represent the $\mp$ SD across stimulus pairs. (D) Network learning performance after 500 training trials for different *CS-US* delays. Bars denoted $\mp$ SD across stimulus pairs.

and the model provides a mechanistic explanation: conditioning worsens with increasing delays because the memory representation of the *CS* is leaky and degrades at longer delays, as shown in fig. 1D.

Extinction and re-acquisition

The model can also account for the phenomenon of extinction. To investigate this, we focus on the case in which the *RNN* only needs to learn a single *CS-US* pair in the delay conditioning task described before. We keep the same trial structure, except that the *US* is not shown at all, and the trial duration is extended (fig. 4A). The latter is important because in extinction, the computation of surprise in equation 22 is triggered t_{wait} seconds after the normal time the *US* would appear, where t_{wait} is the time after which the *US* is no longer expected. Without loss of generality, we set $t_{\text{wait}} = 5$ seconds.

As shown in fig. 4B, the network learns this association with a small number of trials. At this point the extinction regime is introduced by presenting the same *CS* in isolation, and as a result the learned association rapidly disappears from the network (fig. 4B,C).

Figure 4D looks at the phenomenon of re-acquisition where, after a period of extinction, the same *CS-US* pair is reintroduced in training. A common finding in many classical conditioning experiments is that re-acquisition is faster than the initial learning [21]. To test this, we compare
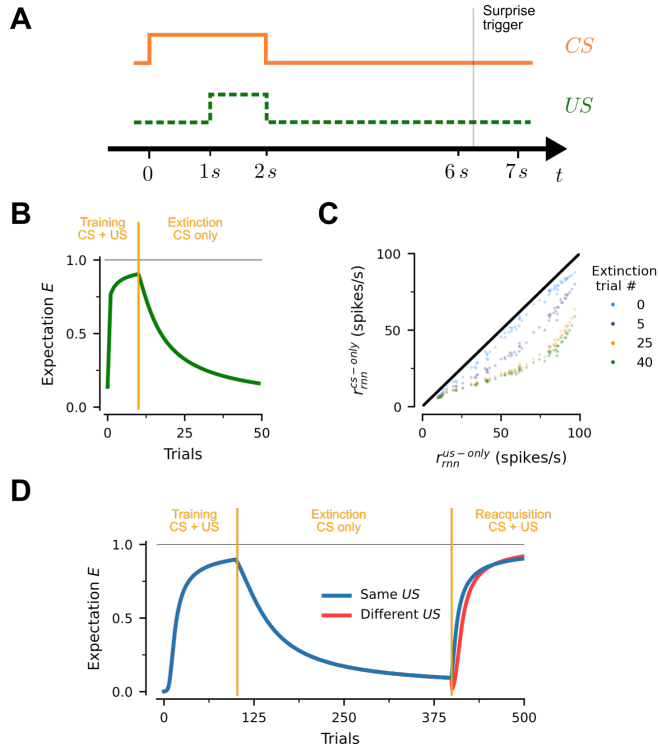
Figure 4: **Extinction and re-acquisition**. (A) Trial structure. In trials where there *US* is not shown, surprise is computed at $t \approx 6$ seconds. (B) Learning and extinction path for the acquisition of a single *CS-US* pair. (C) Evolution of population responses during extinction. Colors denote extinction trial number. Each point compares the firing rate of an associate neuron at that stage of learning for a specific *CS-US* pair when only the *US*, or only the associated *CS* are presented. (D) Learning, extinction and re-acquisition path. Blue line involves an experiment in which the same *CS-US* pair is used in training and re-acquisition. Red line involves an experiment in which a new *US* is used at the re-acquisition phase.

two cases: one in which the same *US* is used during re-acquisition (shown in blue), and one in which a different *US* is used during re-acquisition (shown in red). We find that re-learning an association to the same *US* is faster, therefore accounting for experimental findings on re-acquisition. Furthermore, our network provides a mechanistic explanation: re-acquisition is faster because the responses of the neurons in fig. 4C have not decayed to zero, even though the expectation almost has. Therefore, re-learning is faster to begin with, although the new pattern catches up later.

Phenomena arising from *CS* competition

So far we have focused on experiments in which the network needs to learn one-to-one *CS-US* pairings. However, some of the most interesting findings in conditioning arise when multiple *CS*s are associated with the same *US*.

To explore this, we extend the model to the case in which the network can be exposed to two *CS*s for each *US* (fig. 5A). Now there are two separate *RNN*s of associative neurons, one for each *CS*. Without loss of generality we focus on delay conditioning and therefore, for the sake of simplicity, we remove the short-term memory network and directly feed inputs for the
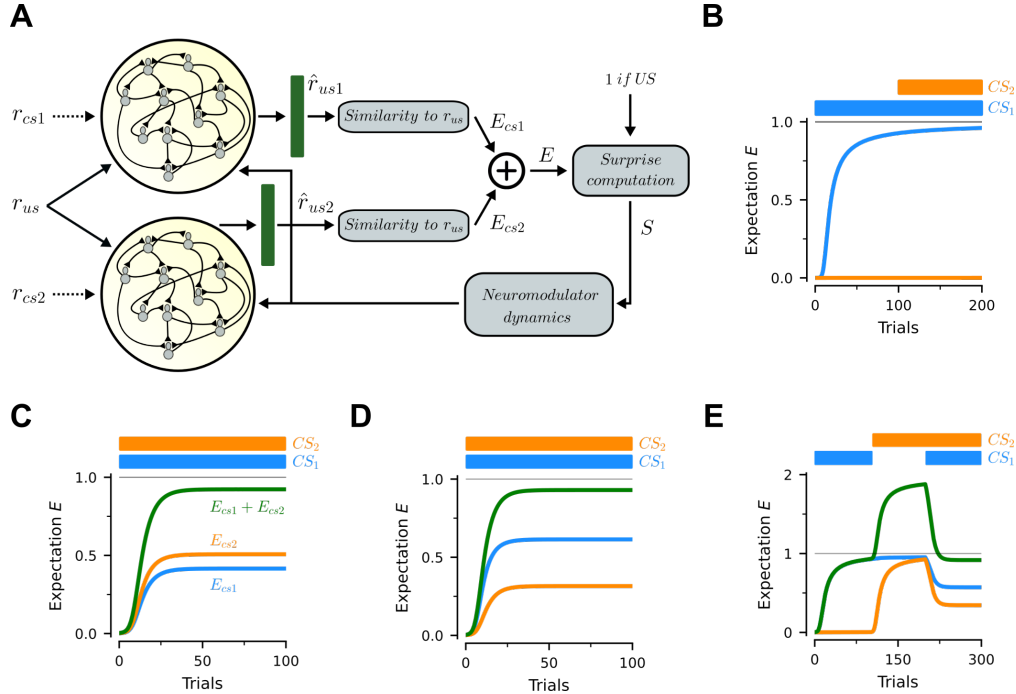
9

Figure 5: **Blocking, overshadowing, saliency and overexpectation**. (A) Model extension to allow for simultaneous presentation of two CSs. Associations for CS_1 and CS_2 are represented in separate populations of associative neurons. The activity of each population is used to separately decode the US and to construct expectations E_{cs1} and E_{cs2}. The overall expectation generated by the two CSs is given by $E = E_{cs1} + E_{cs2}$. Experiments assume that a single association between the US and both CSs has to be learnt. E_{cs1} is the prediction generated by CS_1 alone. E_{cs2} is the prediction generated by CS_2 alone. and $E_{cs1} + E_{cs2}$ is the prediction generated by both cues together. Since the CSs are present throughout the trial, we omit the short-term memory networks from this exercise. (B) Blocking: CS_1 is presented in isolation and fully learns to predict the US before CS_2 is introduced. In this case, CS_2 is blocked from learning to predict the US. (C) Overshadowing: Both CSs are presented from onset and none of them reaches the same conditioning level as when it was presented alone; instead, the sum E of their expectations learns the full association. (D) Saliency effects: similar to (C), but now the relative salience of CS_1 has been increased by scaling up its input vector. As a result, the final conditioning level of CS_1 is consistently higher than the one for CS_2. (D) Overexpectation: CS_1 and CS_2 are conditioned separately. When presented together, E exceeds 1, which leads to a negative learning rate and unlearning.

respective CSs (denoted by r_{cs1} and r_{cs2}). The activity of these populations is used to decode the identity of the US, based on the activity generated by each CS separately. These predictions are then used to generate expectations E_{cs1} and E_{cs2}, which denote the predicted strength generated by each of them when shown in isolation. The total expectation for the US is then given by $E = E_{cs1} + E_{cs2}$. The same logic could be extended to more than two CSs. For all of these experiments, we learn a single association between a pair of CSs and a single US, i.e. $N_{\text{stim}} = 1$.

Figure 5B presents the results for a typical blocking experiment. We first present CS_1 alone for the first 100 trials, resulting in the acquisition of an expectation very close to 1. Subsequently, we start presenting both CSs together. However, the US is already well predicted from CS_1, resulting in small surprises after CS_2 is introduced, and thus an approximate zero learning rate.

Thus, in this setting the model generates the well established phenomenon of blocking.

Figure 5C studies an overshadowing experiment. Here we present both CSs together from the first trial. In this case both of them develop an expectation from the US, but neither individually reaches 1. Instead, it is the sum of their expectations that learns the association. Thus, in this setting the model generates the well established phenomenon of overshadowing. Notice that the expectation stemming from one of the CSs is larger than the other, which can be attributed to randomness in the weight matrix initializations.

Figure 5D investigates the impact of stimulus saliency in CS competition. Salient stimuli receive more attention and generate stronger neural responses than similar but less salient ones [22]. We model relative saliency by multiplying the input vector r_{cs1} of CS_1, the high-saliency cue, by a constant $s_h = 1.2$, while keeping r_{cs2} the same. Otherwise, the task is identical to the case of overshadowing. Consistent with animal experiments, fig. 5D shows that the more salient CS_1 acquires a substantially stronger association with the US than the less salient CS_2. This results from the fact that the more salient stimulus leads to higher firing rates, and thus to stronger pre-synaptic potentials which strengthen learning at those synapses.

Finally, fig. 5E presents the results for a typical overexpectation experiment. Here CS_1 is presented alone for the first 100 trials, CS_2 is then presented alone for the next 100, and starting from trial 200, both CSs are presented together. Since at this point the CSs already have expectations very close to 1, their joint expectation greatly surpasses 1. As a result, surprise is now negative, leading to unlearning of both conditioned responses, up to the point where $E_{cs1} + E_{cs2} \approx 1$.

Contingency and unconditional support

So far we have considered experiments that depend on the temporal contiguity of the CS and US. Another important variable affecting conditioning is contingency; i.e., the probability with which the CS and the US are presented together [23].

To vary the level of contingency, the US is shown in every trial, but the CSs are presented only with some probability, which we vary across experiments. Note that this is not the only way of running contingency conditioning experiments. For example, one could change the contingency by showing the CSs every trial and then only show the US with some probability. This would manipulate the degree of contingency, but also introduce an element of extinction, since there are some trials in which no US follows the CS. We favor the aforementioned experiment because it eliminates this confound.

Figure 6A involves experiments with a single CS which is shown with different probability. Consistent with the animal literature [23], we find that the strength and speed of learning increases with the CS-US contingency.

Figure 6B involves experiments with two independent predictive stimuli. Every trial CS_1 is shown with probability 0.8 and, independently, CS_2 is shown with probability 0.4. Unsurprisingly, we find that the CS with the highest contingency acquires the stronger predictive response. Note that the conditioned responses do not need to add up to 1 in this setting.

Figure 6C,D involves a different probabilistic structure for the CSs. CS_1 is shown every trial with probability 0.8, as in the previous case. But now CS_2 is only shown if CS_1 is present, and with various probability $P(CS_2|CS_1)$. When $P(CS_2|CS_1) = 0.5$, the unconditional probabilities
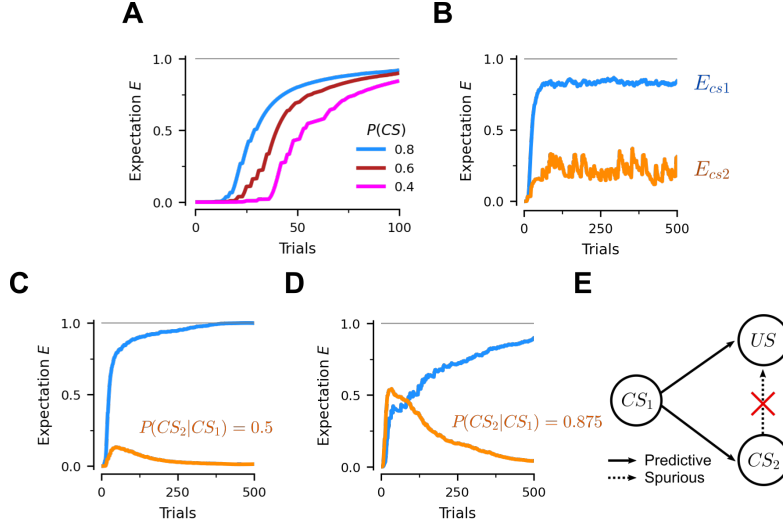
Figure 6: **Contingency and causality**. The US is shown every trial, while the contingency of the CSs is varied. (A) Impact of changing the probability of showing the CS in every trial. Each line depicts the learning path for a different experiment. (B) Experiment with two independent predictive stimuli. In every trial, CS_1 is shown with probability 0.8 and CS_2 is shown with probability 0.4. Blue curve is the expectation acquired by CS_1 when shown by itself. Orange curve is the expectation acquired by CS_2 when shown by itself. (C,D) Experiments with a conditional CS structure. Every trial CS_1 is shown with probability 0.8 and CS_2 is shown only if CS_1 is also present, with probability $P(CS_2|CS_1)$. (E) The network learns to ignore spurious predictors. Since CS_2 is conditionally dependent on CS_1, our network gradually phases out any explanatory power of CS_2, as more evidence that the US is never caused by the CS_2 by itself arrives.

of the two CSs are the same as in fig. 6B, but the associations learnt are different. After an initial acquisition phase, E_{cs2} decays monotonically to zero. More interestingly, the same effect arises if $P(CS_2|CS_1) = 0.875$, where $P(CS2) = 0.7$: even though the two CSs are similarly likely, E_{cs2} decays to zero after initially going toe-to-toe with E_{cs1}. This exemplifies the heavily non-linear behavior of this phenomenon.

To explain this finding, we need to introduce the concept of *unconditional support*. A CS has unconditional support if there are trials when it is presented by itself, which means the network has to rely on it to predict the incoming US. In fig. 6B, both CSs have unconditional support, albeit CS_2's is much lower. This explains both the noisiness in E_{cs2}, which increases each time CS_2 is presented alone, and the fact that $E_{cs2} < E_{cs1}$. However, the situation drastically changes when CS_2 is only presented together with CS_1. Here CS_2 has no unconditional support. Initially, both CSs are conditioned, until the sum of their conditioned responses reaches 1. At that point no more positive surprise is generated for CS_2. When CS_1 is presented alone, $S > 0$ because $E_{cs1} < 1$, which leads to an increase in the E_{cs1} association. When both CSs are presented together, the sum of their conditioned responses is now greater than 1, and therefore $S < 0$ and both conditioned responses drop. As a result, over time E_{cs2} gradually decay to zero. This also explain why E_{cs} takes longer to decay when $P(CS_2|CS_1)$ is high.

In this task, CS_2 is a spurious predictor of the US, since it only appears if CS_1 is shown, and has no additional predictive value conditional on CS_1, as shown in fig. 6E. Essentially, the

network learns to retain the predictive relationship but erase the spurious one. Importantly, we did nothing that would bias the network towards developing this strikingly non-linear effect.

A common fallacy of causal reasoning is known as the *post hoc ergo propter hoc* fallacy [24]. It posits that the temporal proximity of two events is sufficient to infer that the earlier event is a contributing cause of the latter. This can lead to erroneous conclusions, when such temporal proximity is coincidental. In fig. 6C-E, CS_1 is predictive of both CS_2 and the US, but CS_2 is not predictive of the US, despite it preceding it temporally. Therefore, the network can recognize the lack of predictive ability (or unconditional support) of CS_2, resolving the *post hoc* fallacy in this simpler predictive setting. Similar mechanisms might allow the brain to perform more advanced forms of causal reasoning.

Finally, note that compared to other conditioning phenomena, the network takes substantially longer to learn the predictive structure of the task. Combined with the fact that real world data are scarce and often ambiguous, this might explain why such fallacies often persist.

Discussion

The ability to engage in stimulus-stimulus associative learning provides a crucial evolutionary advantage. The cerebral cortex might contribute to this evolutionary edge by exploiting representational [7] and architectural [14] inductive biases present in the cortical microcircuit [10]. We here propose a recurrent neuronal network model of how the cortex can implement stimulus substitution, which allows the same set of neurons to encode multiple stimulus-stimulus associations. The model relies on the properties of two-compartment layer-5 pyramidal neurons, which based on recent experimental findings, we refer to as associative neurons. These neurons can act as coincidence detectors for information about the US arriving at their somatic compartment and information about the CS arriving at their dendritic compartment [11, 12, 14]. Coincidence detection allows for a biologically plausible synaptic plasticity rule that, after learning, results in neurons that would normally fire in the presence of the US to respond in the same manner when the CS is presented. At the population level, this means that the pattern of neural activity corresponding to the CS can be morphed into the one corresponding to the US, leading to stimulus substitution.

Our model accounts for many of most important conditioning phenomena observed in animal experiments, including delay conditioning, trace conditioning, extinction, blocking, overshadowing, saliency effects, overexpectation and contingency effects. The model is able to learn multiple *CS-US* associations with a degree of training that is commensurate with animal experiments. Significantly, the model performs well across a wide variety of conditioning tasks without experiments-specific parameter fine-tuning.

We also show that some influential models of three-factor Hebbian learning rules - Oja's rule [17] and the BCM rule [18] - fail to learn generic stimulus-stimulus associations due to their unsupervised nature. Hebbian rules have demonstrable autoassociative [25] and heteroassociative [26] capabilities, and when augmented with eligibility traces they have been shown to account for neuronal-level reinforcement learning [16, 27, 28]. Still, they struggle with pattern-to-pattern associations when representations are mixed. This is because Hebbian rules are purely unsupervised, and therefore provide no guarantee that the impact of the CS will be eventually shaped

to be identical to the one of the *US*. Instead, network performance heavily depends on implementation details, like training history, task details and stimulus statistics. As a result, decoding from a population encoding several associations is hampered by the fact that activation levels for individual neurons when exposed to the *CS* will more often than not be off from those resulting from exposure to the corresponding *US*.

Related work utilized a predictive learning rule similar to the one used here to account for prospective coding of anticipated stimuli [29]. While prospective coding might also be involved in conditioning, their study differs in several ways. First, their learning rule is timing-dependent; it succeeds in a delayed pair associative learning task, but it would require re-learning when the relative timing of the *US* in relation to the *CS* is variable. In contrast, our learning rule applies to arbitrary task timings. Second, their learning rule lacks gating which, unless strict conditions are met (dendritic and somatic activity conditioned on a stationary Markov chain), leads to reduced responses and even catastrophic forgetting. Furthermore, adding gating is not feasible in their model, because learning needs to bootstrap before the presentation of the delayed stimulus, and gating would inactivate learning at these times.

Several features of the model are worth emphasizing.

First, the proposed *RNN* leverages architectural inductive biases in the form of two-compartment associative neurons. These associative neurons are the most common neuron type in the mammalian cortex [10]. This is likely no coincidence; once evolution stumbled upon their usefulness in predicting external contingencies, it might have favored them. While subcortical [8] and even single-neuron [9] mechanisms for conditioning exist, the mechanism that we propose can handle mixed representations, and thus allow animals with a cerebral cortex to flexibly learn large numbers of associations.

The structure of the associative neuron is ideal for stimulus-stimulus learning. Feedforward inputs, like the *US* representations, arrive near the soma in layer-5 and directly control the neuron's firing rate. Feedback inputs, like the *CS* representations and the activity of other cortical neurons, arrive at the distal dentrites in layer-1 [12]. This compartmentalized structure allows the signals to travel independently, and get associated via a cellular mechanism known as BAC firing [14]. Specifically, it has been shown that these cells implement coincidence detection, whereby feedforward inputs trigger a spike which backpropagates to the distal dendrites and concurrently feedback input arrives at these dendrites, then plateau calcium potentials are initiated in the dendritic compartment [14]. These plateau potentials result in the neuron spiking multiple times subsequently and learning occurs in the distal dendrites, so that feedback inputs can elicit spikes alone in the future, without the need for external information.

Second, a prerequisite for the biological plausiblity of the learning rule used in the model is that backpropagating action potentials to be disentangled from postsynaptic potentials at the dendritic compartment. Only then can the two critical components in our learning rule, $f(V^\mathrm{s})$ and $f(p'V^\mathrm{d})$ in eq. 1 be compared. Since backpropagating action potentials (denoted by $f(V^\mathrm{s})$ in the model) do not need to travel far, they experience minimal attenuation [14] and therefore they maintain some of their high-frequency components, which could be used at synapses to differentiate them from slower postsynaptic potentials (denoted by V^d in the model). As a result, only a static transformation of this last term is needed to compare the two signals. Consequently, the learning rule relies only on information locally available at each synapse, which

is a prerequisite for biological plausibility.

Third, our model suggests multiple functional roles for gating. It limits learning to episodes that appear to have behavioral significance. Gating also prevents drifting of learned associations due to a lack of perfect self-consistency between $f(V^{\mathrm{s}})$ and $f(p'V^{\mathrm{d}})$ in the learning rule [16], which is expected in a biological system subject to noise and approximate computation. In addition, gating provides a critical global reference signal when multiple CSs are available at the same time.

The model also has some limitations to be addressed in future work. Most importantly, it does not account for spontaneous recovery of previously learnt associations after extinction. In our model, extinction stems from the decay of the response of the associate neurons to the CS, a mechanism akin to unlearning, which erases previous learning, and thus does not allow for spontaneous recovery or faster re-acquistion. The extinction mechanism proposed here is complementary to inhibitory learning, the mechanism initially put forth by Pavlov to explain spontaneous recovery.

In the case of experiments with multiple CSs, the model assumes that different neuronal population implements separate RNNs to learn the associations for each of them. Although the two populations interact indirectly through the surprise signals, they each learn to predict the US on their own. The existence of separate populations might be justifiable when the CSs involve different sensory modalities (e.g., sound and vision), or very different spatial locations, but not necessarily when they are presented simultaneously. Extending the model to include differential routing of simultaneously presented stimuli is an open question for future work.

Another direction for future work is to account for more psychological aspects of conditioning by developing a larger model that incorporates other forms of learning and generalization like model-based strategies also thought to take place in the PFC [30], or to allow for context-dependent computation to resolve conflicts among competing stimuli [31]. In these larger models, our network would model the stimulus substitution component.

The model allows to differentiate between conditioning effects that can be accounted by low-level, synaptic plasticity mechanisms, versus other high level explanations. At its core, the model performs stimulus substitution at the neuronal level, via a gradual acquisition process [32–34]. Despite that, the model is still capable of rapid, few-shot learning, especially when the number of associations is small compared to size of the network (fig. 2E). Yet, for rapid learning in more complicated scenarios, fast inference based on prior knowledge might be necessary [35].

Finally, our model suggest an alternative role for representational inductive biases in the form of mixed selectivity, other than readout flexibility [36]: it permits the efficient packing of multiple stimulus-stimulus associations within the same neuronal population, which might confer cortical animals the evolutionary edge.

Methods

RNN of associative neurons

The central element of the model is a RNN of N_{rnn} associative neurons. The goal of the network is to learn to predict the identity of the upcoming US from the presentation of the corresponding

CS, by reproducing the *US* population vector when only the *CS* is presented. Each associative neuron is a two-compartment rate neuron modelled after layer-5 pyramidal cortical neurons [14, 15]. The somatic compartment models the activity of the soma and apical dendrites of the neuron, while the dendritic compartment models the activity of distal dendrites in cortical layer-1. As depicted in fig. 1B, the somatic compartment receives $r_{\mathrm{us}}(t)$ as input, whereas the dendritic compartment receives $\hat{r}_{\mathrm{cs}}(t)$ as well feedback activity from the all the *RNN* units, which is denoted by $r_{\mathrm{rnn}}(t)$.

The instantaneous firing rate of the associative neurons is a sigmoidal function of the somatic voltage V^{s}:

$$r_{\mathrm{rnn}} = \frac{f_{\max}}{1 + \exp\left[-\beta(V^{\mathrm{s}} - V_{1/2})\right]}. \tag{2}$$

This activation function is applied element-wise to the vector V^{s}, which represents the instantaneous somatic voltage in each associative neuron. $f_{\max}$ sets the maximum firing rate of the neuron, β is the slope of the activation function, and $V_{1/2}$ is the voltage level at which half of the maximum firing rate is attained. We set $f_{\max}$ to a reasonable value for cortical neurons, and choose appropriate values for β and $V_{1/2}$ so that the whole dynamic range of the activation function is used and firing rates when somatic input is present are relatively uniform. See Table 1 for a description of all model parameters, and Table S1 for their justification.

The somatic voltages, and thus the firing rates, are determined by the following system of differential equations:

- The associative neurons receive an input current to their dendritic compartments, denoted by I^{d}, which obey:

$$\tau_{\mathrm{s}}\frac{\mathrm{d}I^{\mathrm{d}}}{\mathrm{d}t} = -I^{\mathrm{d}} + W_{\mathrm{cs}}\,\hat{r}_{\mathrm{cs}} + W_{\mathrm{rnn}}\,r_{\mathrm{rnn}} \tag{3}$$

  where W_{rnn} is the matrix of synaptic weights between any pair of associative neurons (dimension: $N_{\mathrm{rnn}} \times N_{\mathrm{rnn}}$), W_{cs} is the matrix of synaptic weights for the *CS* input (dimension: $N_{\mathrm{rnn}} \times N_{\mathrm{inp}}$), and τ_{s} is the synaptic time constant.

- The dynamics of the voltage in the dendritic compartments V^{d} are given by:

$$\tau_{\mathrm{l}}\frac{\mathrm{d}V^{\mathrm{d}}}{\mathrm{d}t} = -V^{\mathrm{d}} + I^{\mathrm{d}}; \tag{4}$$

  i.e. it is a low-pass filtered version of the dendritic current I^{d} with the leak time constant τ_{l}. For simplicity, voltages and currents are dimensionless in our model. Therefore the leak resistance of the dendritic compartment is also dimensionless and set to unity.

- The voltages of the somatic compartments, denoted by V^{s}, are given by:

$$C\frac{\mathrm{d}V^{\mathrm{s}}}{\mathrm{d}t} = -g_L V^{\mathrm{s}} - g_D(V^{\mathrm{s}} - V^{\mathrm{d}}) + I^{\mathrm{s}} \tag{5}$$

  where C is the somatic membrane capacitance, g_L is the leak conductance, g_D is the conductance of the coupling from the dendritic to the somatic compartment, and I^{s} is a vector of input currents to the somatic compartments. Note that this specification assumes that the time constant for the somatic voltage is one, or equivalently, that it is included in C.

16

- The vector I^{s} of input currents to the somatic compartment is given by:

$$I^{\mathrm{s}} = g_{\mathrm{e}} \odot (E_{\mathrm{e}} - V^{\mathrm{s}}) + g_{\mathrm{i}} \odot (E_{\mathrm{i}} - V^{\mathrm{s}}) \tag{6}$$

  where g_{e} and g_{i} are vectors describing the time-varying excitatory and inhibitory conductances of the inputs, E_{e} and E_{i} are the reversal potentials for excitatory and inhibitory inputs, and $\odot$ denotes the Hadamard (element-wise) product.

- The vectors of excitatory and inhibitory conductances g_{e} and g_{i} for the somatic compartment are described, respectively, by the following two equations:

$$\tau_{\mathrm{s}} \frac{\mathrm{d}g_{\mathrm{e}}}{\mathrm{d}t} = -g_{\mathrm{e}} + [W_{\mathrm{us}}]_+ \, r_{\mathrm{us}} \tag{7}$$

  and

$$\tau_{\mathrm{s}} \frac{\mathrm{d}g_{\mathrm{i}}}{\mathrm{d}t} = -g_{\mathrm{i}} + [-W_{\mathrm{us}}]_+ \, r_{\mathrm{us}} + g_{\mathrm{inh}} \tag{8}$$

  where W_{us} is a matrix describing the synaptic weights for the US inputs to the somatic compartments (dimension: $N_{\mathrm{rnn}} \times N_{\mathrm{inp}}$), τ_{s} is the same synaptic time constant used in equation 3, g_{inh} is a constant inhibitory conductance of all associative neurons, and $[.]_+$ is the rectification function applied element-wise.

The model implicitly assumes zero resting potentials for the somatic and dendritic compartments. In addition, we assume that there is no input to the RNN between trials, and that the inter-trial interval is sufficiently long so that the variables controlling activity in the associative neurons reset to zero between trials. The differential equations describing activity within trials are simulated using the forward Euler method with time setp $\Delta t = 1$ ms.

At the beginning of the experiment, all synaptic weight matrices are randomly initialised, independently for each entry, using a normal distribution with mean 0 and standard deviation $1/\sqrt{N_{\mathrm{rnn}}}$, as is standard in the literature. Note that since associative neurons are pyramidal cells, the elements of W_{rnn} are restricted to positive values; hence we use the absolute value of those random weights.

W_{us} stays fixed for the entire experiment. W_{rnn} and W_{cs} are plastic and updated using the learning rules described next.

Synaptic plasticity rule

We utilize a synaptic plasticity rule inspired by [11, 12, 14], where the firing rate of the somatic compartment in the presence of the US acts like a target signal for learning the weights W_{rnn} and W_{cs} (see [15] for the initial spike-based learning rule, and [37] for the rate-based formulation). The learning rule modifies these synaptic weights so that, after learning, CS inputs can predict the responses of the RNN to the USs.

Consider the synaptic weights from input neuron j to associative neuron i, for either the RNN or the CS inputs. The weights are updated continuously during the trial using the following rule:

$$\Delta W_{ij} = \eta(S) \left[f(V_i^{\mathrm{s}}) - f(p' \, V_i^{\mathrm{d}}) \right] P_j \tag{9}$$

Parameter	Value	Units	Description
N_{stim}	16		Number of CS-USs pairs to be learnt
t_{trial}	2	s	Trial duration
$t_{\text{cs-off}}$	2	s	Time in the trial at which CS disappears
$t_{\text{us-on}}$	1	s	Time in the trial at which US appears
N_{inp}	20		Stimuli input vector length
H_{d}	8		Minimal Hamming distance between behavioral stimulus vectors
N_{rnn}	64		Number of associative neurons
f_{max}	100	spikes/s	Maximum firing rate
β	2		Steepness of activation function
$V_{1/2}$	1.5		Input level for 50 % of the maximum firing rate
τ_{s}	100	ms	Synaptic time constant
τ_{l}	20	ms	Leak time constant of dendritic compartment of associative neurons
C	2	ms	Capacitance of somatic compartment of associative neurons
g_L	0.1		Leak conductance of somatic compartment of associative neurons
g_D	0.2		Conductance from dendritic to somatic compartment
g_{inh}	3/8		Constant inhibitory conductance
E_{e}	14/3		Excitatory synaptic reversal potential
E_{i}	−1/3		Inhibitory synaptic reversal potential
a	0.95		Constant for deviation of the learning rule from self-consistency
τ_{r}	200	ms	Dopamine release time constant
τ_{u}	300	ms	Dopamine uptake time constant
η_0	$5 * 10^{-3}$		Baseline learning rate
Δt	1	ms	Euler integration step size

Table 1: **Model parameter values**. These values apply to all simulations, unless otherwise stated. Note that voltages, currents, and conductances are assumed unitless in the text; therefore capacitances have the same units as time constants.

where $\eta(S)$ is a variable learning rate that depends on the instantaneous level of a surprise signal S, p' is an attenuation constant derived below, and P_j is the postsynaptic potential in input neuron j.

The postsynpactic potential P_j has a simple closed form solution detailed in [37]. In particular, it is a low-passed filtered version of the neuron's firing rate, so that

$$P_j(t) = H(t) * r_j(t), \tag{10}$$

where $*$ denotes the convolution operator, and H is the transfer function given by

$$H(t) = \frac{1}{\tau_{\text{l}} - \tau_{\text{s}}} \left[\exp(-\frac{t}{\tau_{\text{l}}}) - \exp(-\frac{t}{\tau_{\text{s}}}) \right] u(t) \tag{11}$$

and $u(t)$ is the Heaviside step function that takes a value of 1 for $t > 0$ and a value of 0 otherwise.

As noted in [37], for constant η the learning rule is a predictive coding extension of the classical Hebbian rule. When η is controlled by a surprise signal, as in our model, it can be thought of a predictive coding extension of a three-factor Hebbian rule [28, 38].

Importantly, all of the terms in the learning rule are available at the synapses in the dendritic compartment, making this a local, biologically plausible learning rule. The firing rate of the neuron $f(V_i^s)$ is available due to backpropagation of action potentials [14]. $f(p'V_i^d)$ is a constant function of the local voltage V_i^d computed locally in the dendritic compartment even when the somatic input is present. By definition, postsynaptic potentials are available at the synapse.

There are a total number of N_{train} training trials, divided among all *CS-US* pairs. After each training trial we measure the state of the *RNN* off-line by inputing one r_{cs} at a time without the *US*, keeping the network weights constant, and measuring the output produced by the model at that stage of the learning process.

Convergence of synaptic plasticity rule

To understand how and why the learning rule works, it is useful to characterize the somatic voltages, and thus their associated firing rates, in different trial conditions.

Consider first the case in which only the *CS* is presented, so the associative neurons only receive dendritic input. In this case the somatic voltages converge to a steady-state given by

$$V^{\text{ss}} = \frac{g_D}{g_D + g_L} V^{\text{d}}. \tag{12}$$

In other words, the somatic voltages converge simply to an attenuated level of the dendritic voltages, with the level of attenuation given by $p = \frac{g_D}{g_D + g_L}$. In this case, the firing rates of the associative neurons converge to

$$r_{\text{rnn}}^{\text{cs-only}} = f(V^{\text{ss}}) \tag{13}$$

This follows from the fact that the dendritic voltage is determined only by equations 3 and 4, and thus is not affected by the state of the somatic compartment, and by the fact that in the absence of *US* input $I^s = 0$. The result then follows immediately from equation 5.

Next consider the case in which only the *US* is presented. In this case equations 3 and 4 imply that $V^{\text{d}} = 0$, and it then follows from equations 5 and 6 that the steady-state somatic voltage, when $I^s = 0$, is given by

$$V^{\text{eq}}(t) = \frac{g_e E_e + g_i E_i}{g_e + g_i} \tag{14}$$

and that the firing rates of the associative neurons become

$$r_{\text{rnn}}^{\text{us-only}} = f(V^{\text{eq}}). \tag{15}$$

Finally consider the case in which the associative neurons receive input from both the *CS* and the *US*. We follow [29] to derive the steady-state solution for the somatic voltage in this case. Provided inputs to the circuit, which are in behavioral timescales, change slower than the membrane time constant ($C/g_L = 20\,\text{ms}$), equation 5 reaches a steady-state given by

$$V^{\text{s}}(t) \approx \kappa V^{\text{ss}} + (1 - \kappa) V^{\text{eq}}, \tag{16}$$

where $\kappa(t) = \frac{g_D + g_L}{g_D + g_L + g_e + g_i} \in (0, 1]$ performs a linear interpolation between the steady-state levels

reached where only the *CS* or the *US* are presented.

Practically, when there is no *US*-input, V^{ss} slightly precedes V^s due to the non-zero dendritic-to-somatic coupling delays, resulting in slight overestimation of the firing rate upon *CS* presentation. This can be accounted for by introducing an additional small attenuation, so that $p' = a\frac{g_D}{g_D+g_L} = ap$ in equation 9, with $a = 0.95$.

Learning is driven by a comparison of the firing rates of the associative neurons in the presence of both the *CS* and the *US*, and the firing rates if they only receive input from the *CS*. Importantly, this can happen online and without the need for separate learning phases, because an estimate of the latter can be formed in the dendritic compartment at all times. Learning is achieved by modifying W_{rnn} and W_{cs} to minimize this difference. We can use the expressions derived in the previous paragraphs to see why the synaptic learning rule converges to synaptic weights for which $r_{rnn}^{cs\text{-}only} = r_{rnn}^{both}$.

Take the case in which associative neurons underestimate the activity generated by the *US* inputs when exposed only to the *CS* (i.e. $V^{ss} < V^{eq}$). In this case, $V^{ss} < V^s < V^{eq}$ and $I^s > 0$. Then from equation 9 we find that $\Delta w > 0$, leading to a futures increase in associative neuron activity in response to the *CS*.

The same logic applies in opposite case, where the associative neurons overestimate the activity generated by the *US* inputs when exposed only to the *CS*. In this case, $V^{ss} > V^s > V^{eq}$ and $I^s < 0$, which leads to a future decrease in associative neuron activity in response to the *CS*.

Given enough training, this leads to a state where $V^{ss} \approx V^{eq}$ and at which learning stops ($\Delta w \approx 0$). When this happens, we have that

$$r_{rnn}^{cs\text{-}only} = f(V^{ss}) \approx f(V^{eq}) = r_{rnn}^{both}, \tag{17}$$

so that the *RNN* responses to the *CS* become fully predictive of the activity generated by the *US*, when presented by themselves.

US decoding

Up to this point the model has been faithful to the biophysics of the brain. The next part of the model is designed to capture the variable learning rate η in equation 9, and thus is more conceptual in nature. Our goal here is simply to provide a plausible model of the factors affecting the learning rates for the *RNN*. As illustrated in fig. 1C, this part of the model involves three distinct computations: decoding the *US* from the *RNN* activity, computing expectations about upcoming *US*s, and computing the surprise signal S.

The brain must have a way to decode the upcoming *US*, or its presence, from the population activity in the *RNN* at any point during the trial. This prediction is represented by the time-dependent vector $\hat{r}_{us}(t)$. For the purposes of our model, we will use the optimal linear decoder D (dimension: $N_{rnn} \times N_{inp}$), so that

$$\hat{r}_{us}(t) = r_{rnn}(t)^\intercal D. \tag{18}$$

The optimal linear decoder D is constructed as follows. First, for each *US* $i = 1, ..., N_{stim}$ define the row vector ϕ_i describing the steady-state firing rate the each associative neuron that

arises when it is presented alone. Then define an activity matrix Φ by stacking vertically these N_{stim} row vectors (dimension: $N_{\text{stim}} \times N_{\text{rnn}}$). Φ is built using the initial random weights W_{rnn}, before learning has taken place. Second, define a target matrix T (dimension: $N_{\text{stim}} \times N_{\text{inp}}$) to be the row-wise concatenated set of US input vectors r_{us}. Then, if D perfectly decodes the US from the RNN activity, when only the USs are presented, we must have that

$$\Phi D = T. \tag{19}$$

It then follows that

$$D = \Phi^+ T, \tag{20}$$

where $^+$ denotes the Moore-Penrose matrix inverse. A desirable property of the Moore-Penrose inverse is that if equation 20 has more than one solutions, it provides the minimum norm solution, which results in the smoothest possible decoding.

Note that the decoder, which could be implemented in any downstream brain area requiring information about USs, is completely independent of the input representations of the CSs. Instead, it is determined before learning given only knowledge of the USs, and is kept fixed throughout training.

US expectation estimation

Since the USs are primary reinforcers, it is reasonable to assume that their representations, r_{us}^i for $i = 1, ..., N_{\text{stim}}$, are stored somewhere in the brain. Then an expectation for each US can be formed by

$$E^i(t) = \exp(-\kappa \|\hat{r}_{\text{us}}(t) - r_{\text{us}}^i\|^2), \tag{21}$$

where $\|\hat{r}_{\text{us}}(t) - r_{\text{us}}^i\|$ is Euclidean distance between the stored and the decoded representations for each US at time t, and κ controls the steepness of the Gaussian kernel. Recognizing that the ability to discriminate these patterns increases with the Hamming distance H_{d}, we set the precision to be inversely proportional to H_{d} i.e. $\kappa = \left(\frac{8}{H_{\text{d}}}\right)^2$.

Note that E^i takes values between 0 and 1, and equals 1 only when the US is perfectly decoded (i.e., when $\hat{r}_{\text{us}} = r_{\text{us}}^i$). Thus, E^i can be interpreted as a probabilistic estimate for each US that is computed throughout the trial. To simplify the notation, we denote the expectation for the US associated with the trial as E.

Surprise based learning rates

The learning rule in equation 9 is gated by a well-documented surprise signal [19]. This surprise signal diffuses across the brain, and activates learning in the RNN.

For each US the following surprise signal is computed throughout the trial:

$$S^i(t) = \delta(t - t_{\text{trig}}) \left(\mathbb{1}_{US^i} - E^i(t - t_{\text{syn}})\right), \tag{22}$$

where $\mathbb{1}_{US^i}$ is an indicator function for the presence of US-i, δ is the Dirac delta function and t_{trig} the time a surprise signal is triggered. In trials where the US appears, we set $t_{\text{trig}} = t_{\text{us-on}} + t_{\text{syn}}$, where $t_{\text{syn}} = 2 * \tau_{\text{s}} = 200\, ms$ is a synaptic transmission delay for the detection of the US

which matches well perceptual delays [39]. The expectation E^i also lags by the same amount, representing synaptic delays from the associative network to the surprise computation area. As can be seen in eq. (22), the more the US is expected upon its presentation, the lower the surprise. In extinction trials, we set $t_{\text{trig}} = t_{\text{us-on}} + t_{\text{syn}} + t_{\text{wait}}$, where t_{wait} is a time after which a US is no longer expected to arrive. The overall surprise signal is given by:

$$S = \sum_i S^i. \tag{23}$$

The surprise signal S gives rise to neuromodulator release and uptake which determine the learning rate η. We assume that separate neuromodulators are at work for positive and negative surprise, and that they follow double-exponential dynamics [40].

Consider the case of positive surprise. The released and uptaken neuromodulator concentration C_{r}^+ and C_{u}^+ are given by:

$$\tau_{\text{r}} \frac{\mathrm{d}C_{\text{r}}^+}{\mathrm{d}t} = -C_{\text{r}}^+ + [S]_+ \tag{24}$$

and

$$\tau_{\text{u}} \frac{\mathrm{d}C_{\text{u}}^+}{\mathrm{d}t} = -C_{\text{u}}^+ + C_{\text{r}}^+ \tag{25}$$

where τ_{r} and τ_{u} are the neuromodulator release and uptake time constants respectively, chosen to match the dopamine dynamics in fig. 1B in [40].

Negative surprise is controlled by a different neuromodulator, described by the following analogous dynamics:

$$\tau_{\text{r}} \frac{\mathrm{d}C_{\text{r}}^-}{\mathrm{d}t} = -C_{\text{r}}^- + [-S]_+ \tag{26}$$

and

$$\tau_{\text{u}} \frac{\mathrm{d}C_{\text{u}}^-}{\mathrm{d}t} = -C_{\text{u}}^- + C_{\text{r}}^- \tag{27}$$

The neuromodulator uptake concentrations control the learning rate:

$$\eta = \eta_0 \ (C_{\text{u}}^+ - C_{\text{u}}^-), \tag{28}$$

where η_0 is the baseline learning rate.

CS short-term memory circuit

We now describe the short-term memory network used to maintain the $\hat{r}_{\text{cs}}$ representation that serves as input to the RNN.

To obtain a circuit that can maintain a short-term memory through persistent activity in the order of seconds [41], we train a separate recurrent neural network of point neurons using backpropagation through time (BPTT). These networks have been deemed to not be biologically plausible (although see [42]). However, for the purposes of our model we are only interested in the end product of a short-term memory circuit, and not in how the brain acquired such a circuit. Thus, BPTT provides an efficient means of accomplishing this goal.

The memory circuit contains 64 neurons, and the vector of their firing rates r_{mem} obeys:

$$\tau_{\text{s}} \frac{\mathrm{d}r_{\text{mem}}}{\mathrm{d}t} = -r_{\text{mem}} + [W_{\text{mem}} \, r_{\text{mem}} + W_{\text{inp}} \, r_{\text{cs}} + b + n_{\text{mem}}]_+ \tag{29}$$

where W_{mem} is a matrix with the connection weights between the memory neurons (dimension: 64×64), W_{inp} is a matrix of connection weights for the incoming CS inputs to the memory net (dimension: $64 \times N_{\mathrm{inp}}$), τ_{s} is the same synaptic time constant described above, b is a unit-specific bias vector, and n_{mem} is a vector of IID Gaussian noise with zero mean and variance 0.01 added during training. A linear readout of the activity of the memory network provides the memory representation:

$$\hat{r}_{\mathrm{cs}} = W_{\mathrm{out}} \, r_{\mathrm{mem}}, \tag{30}$$

where W_{out} is a readout matrix (dimension: $N_{\mathrm{inp}} \times 64$).

The weight matrices W_{mem}, W_{inp}, and W_{out}, as well as the bias vector b, are trained as follows. Every trial lasts for 3 seconds. On trial onset, a Boolean vector r_{cs} is randomly generated and provided as input to the network. The CS input is provided for a random duration drawn uniformly from $[0.5, 2]$ seconds. The network is trained to output r_{cs} at all times for trials that are 3 seconds long. We train the network for a total of 10^7 trials in batches of 100. We use mean square error loss at the output, with a grace period 200 ms at the beginning of the trial where errors are not penalised. We optimise using Adam [43] with default parameters (decay rates for first and second moments 0.9 and 0.999 respectively, learning rate 0.001). To facilitate BPTT, which does not scale well with the number of timepoints, we train the memory network using a time step of $10 * \Delta t$.

Author contributions P.V. conceived the project, developed the model, performed analyses and wrote the initial draft of the manuscript. A.R. supervised the research and provided funding. A.R. and P.V. wrote the final version of the manuscript.

Data and code availability All code along with data to replicate the results will be shared upon acceptance.

References

[1] Jenkins HM, Moore BR. The form of the auto-shaped response with food or water reinforcers. Journal of the Experimental Analysis of Behavior. 1973;20(2):163–181. doi:10.1901/jeab.1973.20-163.

[2] Dai J, Sun QQ. Learning induced neuronal identity switch in the superficial layers of the primary somatosensory cortex; 2023. Available from: `http://dx.doi.org/10.1101/2023.08.30.555603`.

[3] Sutton RS, Barto AG. A temporal-difference model of classical conditioning. In: Proceedings of the ninth annual conference of the cognitive science society. Seattle, WA; 1987. p. 355–378.

[4] Klopf H. A neuronal model of classical conditioning. Psychobiology. 1988;16:85—-125. doi:10.3758/BF03333113.

[5] Balkenius C, Morén J. Computational Models of Classical Conditioning: A Comparative Study; 1998. Available from: `http://www.lucs.lu.se/People/Christian.Balkenius/PostScript/LUCS62.pdf`.

[6] Izhikevich EM. Solving the Distal Reward Problem through Linkage of STDP and Dopamine Signaling. Cerebral Cortex. 2007;17(10):2443–2452. doi:10.1093/cercor/bhl152.

[7] Rigotti M, Barak O, Warden MR, Wang XJ, Daw ND, Miller EK, et al. The importance of mixed selectivity in complex cognitive tasks. Nature. 2013;497(7451):585–590. doi:10.1038/nature12160.

[8] Christian KM, Thompson RF. Neural Substrates of Eyeblink Conditioning: Acquisition and Retention. Learning & Memory. 2003;10(6):427–455. doi:10.1101/lm.59603.

[9] Gershman SJ, Balbi PE, Gallistel CR, Gunawardena J. Reconsidering the evidence for learning in single cells. eLife. 2021;10. doi:10.7554/elife.61907.

[10] Nieuwenhuys R. The neocortex. An overview of its evolutionary development, structural organization and synaptology. Anatomy and Embryology. 1994;190(4). doi:10.1007/bf00187291.

[11] Doron G, Shin JN, Takahashi N, Drüke M, Bocklisch C, Skenderi S, et al. Perirhinal input to neocortical layer 1 controls learning. Science. 2020;370(6523):eaaz3136. doi:10.1126/science.aaz3136.

[12] Larkum M. A cellular mechanism for cortical associations: an organizing principle for the cerebral cortex. Trends in Neurosciences. 2013;36(3):141–151. doi:10.1016/j.tins.2012.11.006.

[13] Shin JN, Doron G, Larkum ME. Memories off the top of your head. Science. 2021;374(6567):538–539. doi:10.1126/science.abk1859.

[14] Larkum ME, Zhu JJ, Sakmann B. A new cellular mechanism for coupling inputs arriving at different cortical layers. Nature. 1999;398(6725):338–341. doi:10.1038/18686.

[15] Urbanczik R, Senn W. Learning by the Dendritic Prediction of Somatic Spiking. Neuron. 2014;81(3):521–528. doi:10.1016/j.neuron.2013.11.030.

[16] Urbanczik R, Senn W. Reinforcement learning in populations of spiking neurons. Nature Neuroscience. 2009;12(3):250–252. doi:10.1038/nn.2264.

[17] Oja E. Simplified neuron model as a principal component analyzer. Journal of Mathematical Biology. 1982;15(3):267–273. doi:10.1007/bf00275687.

[18] Bienenstock E, Cooper L, Munro P. Theory for the development of neuron selectivity: orientation specificity and binocular interaction in visual cortex. The Journal of Neuroscience. 1982;2(1):32–48. doi:10.1523/jneurosci.02-01-00032.1982.

[19] Gerstner W, Lehmann M, Liakoni V, Corneil D, Brea J. Eligibility Traces and Plasticity on Behavioral Time Scales: Experimental Support of NeoHebbian Three-Factor Learning Rules. Frontiers in Neural Circuits. 2018;12. doi:10.3389/fncir.2018.00053.

[20] Schneiderman N, Gormezano I. Conditioning of the nictitating membrane of the rabbit as a function of CS-US interval. Journal of Comparative and Physiological Psychology. 1964;57(2):188–195. doi:10.1037/h0043419.

[21] Napier RM, Macrae M, Kehoe EJ. Rapid reacquisition in conditioning of the rabbit's nictitating membrane response. Journal of Experimental Psychology: Animal Behavior Processes. 1992;18(2):182–192. doi:10.1037/0097-7403.18.2.182.

[22] Gottlieb JP, Kusunoki M, Goldberg ME. The representation of visual salience in monkey parietal cortex. Nature. 1998;391(6666):481–484. doi:10.1038/35135.

[23] Rescorla RA. Probability of shock in the presence and absence of cs in fear conditioning. Journal of Comparative and Physiological Psychology. 1968;66(1):1–5. doi:10.1037/h0025984.

[24] Hamblin CL. Fallacies. London, England: Methuen young books; 1970.

[25] Hopfield JJ. Neural networks and physical systems with emergent collective computational abilities. PNAS. 1982;79:2554–2558.

[26] Sompolinsky H, Kanter I. Temporal Association in Asymmetric Neural Networks. Physical Review Letters. 1986;57(22):2861–2864. doi:10.1103/physrevlett.57.2861.

[27] Vasilaki E, Frémaux N, Urbanczik R, Senn W, Gerstner W. Spike-Based Reinforcement Learning in Continuous State and Action Space: When Policy Gradient Methods Fail. PLoS Computational Biology. 2009;5(12):e1000586. doi:10.1371/journal.pcbi.1000586.

[28] Frémaux N, Sprekeler H, Gerstner W. Functional Requirements for Reward-Modulated Spike-Timing-Dependent Plasticity. Journal of Neuroscience. 2010;30(40):13326–13337. doi:10.1523/jneurosci.6249-09.2010.

[29] Brea J, Gaál AT, Urbanczik R, Senn W. Prospective Coding by Spiking Neurons. PLoS Computational Biology. 2016;12(6):e1005003. doi:10.1371/journal.pcbi.1005003.

[30] Wang JX, Kurth-Nelson Z, Kumaran D, Tirumala D, Soyer H, Leibo JZ, et al. Prefrontal cortex as a meta-reinforcement learning system. Nature Neuroscience. 2018;21(6):860–868. doi:10.1038/s41593-018-0147-8.

[31] Mante V, Sussillo D, Shenoy KV, Newsome WT. Context-dependent computation by recurrent dynamics in prefrontal cortex. Nature. 2013;503(7474):78–84. doi:10.1038/nature12742.

[32] Thorndike EL. Animal intelligence: An experimental study of the associative processes in animals. The Psychological Review: Monograph Supplements. 1898;2(4):i–109. doi:10.1037/h0092987.

[33] Rescorla RA, Wagner AR. A theory of Pavlovian conditioning: Variations in the effectiveness of reinforcement and nonreinforcement. Current research and theory. 1972; p. 64–99.

[34] Sutton RS, Barto AG. Toward a modern theory of adaptive networks: Expectation and prediction. Psychological Review. 1981;88(2):135–170. doi:10.1037/0033-295x.88.2.135.

[35] Lake BM, Ullman TD, Tenenbaum JB, Gershman SJ. Building machines that learn and think like people. Behavioral and Brain Sciences. 2016;40:e253. doi:10.1017/s0140525x16001837.

[36] Fusi S, Miller EK, Rigotti M. Why neurons mix: high dimensionality for higher cognition. Current Opinion in Neurobiology. 2016;37:66–74. doi:10.1016/j.conb.2016.01.010.

[37] Vafidis P, Owald D, D'Albis T, Kempter R. Learning accurate path integration in ring attractor models of the head direction system. eLife. 2022;11:e69841. doi:10.7554/eLife.69841.

[38] Frémaux N, Gerstner W. Neuromodulated Spike-Timing-Dependent Plasticity, and Theory of Three-Factor Learning Rules. Frontiers in Neural Circuits. 2016;9. doi:10.3389/fncir.2015.00085.

[39] Picton TW. The P300 Wave of the Human Event-Related Potential. Journal of Clinical Neurophysiology. 1992;9(4):456–479. doi:10.1097/00004691-199210000-00002.

[40] Cragg SJ, Hille CJ, Greenfield SA. Dopamine Release and Uptake Dynamics within Nonhuman Primate StriatumIn Vitro. The Journal of Neuroscience. 2000;20(21):8209–8217. doi:10.1523/jneurosci.20-21-08209.2000.

[41] Wang XJ. Synaptic reverberation underlying mnemonic persistent activity. Trends in Neurosciences. 2001;24(8):455–463. doi:10.1016/s0166-2236(00)01868-3.

[42] Greedy W, Zhu HW, Pemberton J, Mellor J, Ponte Costa R. Single-phase deep learning in cortico-cortical networks. Advances in Neural Information Processing Systems. 2022;35:24213–24225.

[43] Kingma D, Ba J. Adam: A Method for Stochastic Optimization. International Conference on Learning Representations. 2014;.

[44] Gerstner W, Kistler WM, Naud R, Paninski L. Neuronal dynamics. Cambridge, England: Cambridge University Press; 2014.

[45] Stringer SM, Trappenberg TP, Rolls ET, de Araujo IET. Self-organizing continuous attractor networks and path integration: one-dimensional models of head direction cells. Network: Computation In Neural Systems. 2002;13(2):217–242.

Supplemental Information

How does the *RNN* learn?

In the main text, we've shown that the network is able to learn complex delay conditioning tasks using relatively few trials. In this section we explore in more detail the mechanisms through which the network solves the problem.

Figure S1 shows how the activity of the associative neurons changes with training. It compares firing rates in response only to the *CS*s (top), in response only to the associated *US*s (middle), or in response to the full trial in which both are presented (bottom). Several things are worth noticing.

First, the right column depicts the activity of the network after it has learnt the delay conditioning task. At this stage, the activity patterns in response to only the *CS* or only the *US* are very similar. This makes it possible to decode the upcoming *US* using only the activity in the network in response to the associated *CS*.

Second, the network learns mixed stimulus representations. This is important since there is evidence that the associative areas of the prefrontal cortex use this type of mixed coding [7].

Third, the pattern of activity in response to only the *US* is unchanged by learning. This follows from the fact that in this case the response of the associative neurons is driven only by the input r_{us} to the somatic compartment and the synaptic weights W_{us} are not updated with training.

Fourth, the activity pattern in response to both the *CS* and the *US*, is very similar to the response to the *US* alone, irrespective of the stage of learning. This is because the firing rate in our model is mainly controlled by the *US*, while later in learning the *CS* would induce the same response anyway. Overall, the learning rule modifies the *CS* weights so that the *CS* inputs are able to generate the representation of the *US* both when the *CS* is presented by itself, and when presented together with the *US*.

Figure S2 provides further insight into the inner workings of the model. Each panel depicts the dynamics of a model component within a training trial. Columns denote different stages of training. Recall that the learning rule between associative neuron i and input neuron j is the product of three terms: a surprise modulated learning rate $\eta(S)$, the presynaptic potential in the input neuron P_j, and the neuron-specific firing rate error term $\left[f(V_i^{\mathrm{s}}) - f(p'\, V_i^{\mathrm{d}}) \right]$.

Consider the last term first. $f(V_i^{\mathrm{s}})$ is the firing rate of associative neuron i, which is determined by its somatic voltage V_i^{s}. $f(p'\, V_i^{\mathrm{d}})$ is the (approximate) counterfactual firing rate that would occur if the *CS* were presented by itself. When the *US* is presented it dominates the activity of the associative neurons and thus the firing rate in the presence of both stimuli is similar to what would have been in the presence of only the *US*. As a result, for the *RNN* to be able to predict the *US* in response to only the *CS*, it has to be the case that $f(p'\, V_i^{\mathrm{d}}) \approx f(V_i^{\mathrm{s}})$. The learning rule implements a gradient like rule by increasing the *CS* input weights when $f(p'\, V_i^{\mathrm{d}}) < f(V_i^{\mathrm{s}})$, and decreasing them when the opposite is true. As shown in the third row of fig. S2, these two variables are unrelated early in training, but converge to the same pattern as learning progresses.

Next consider the surprise modulated learning rate $\eta(S)$. Gating the learning rate by surprise is critical, as it provides a global reference signal crucial when there are more than one predictive *CS*s available. Furthermore, biological neurons may not be able to compute $f(p'\, V_i^{\mathrm{d}})$ exactly at
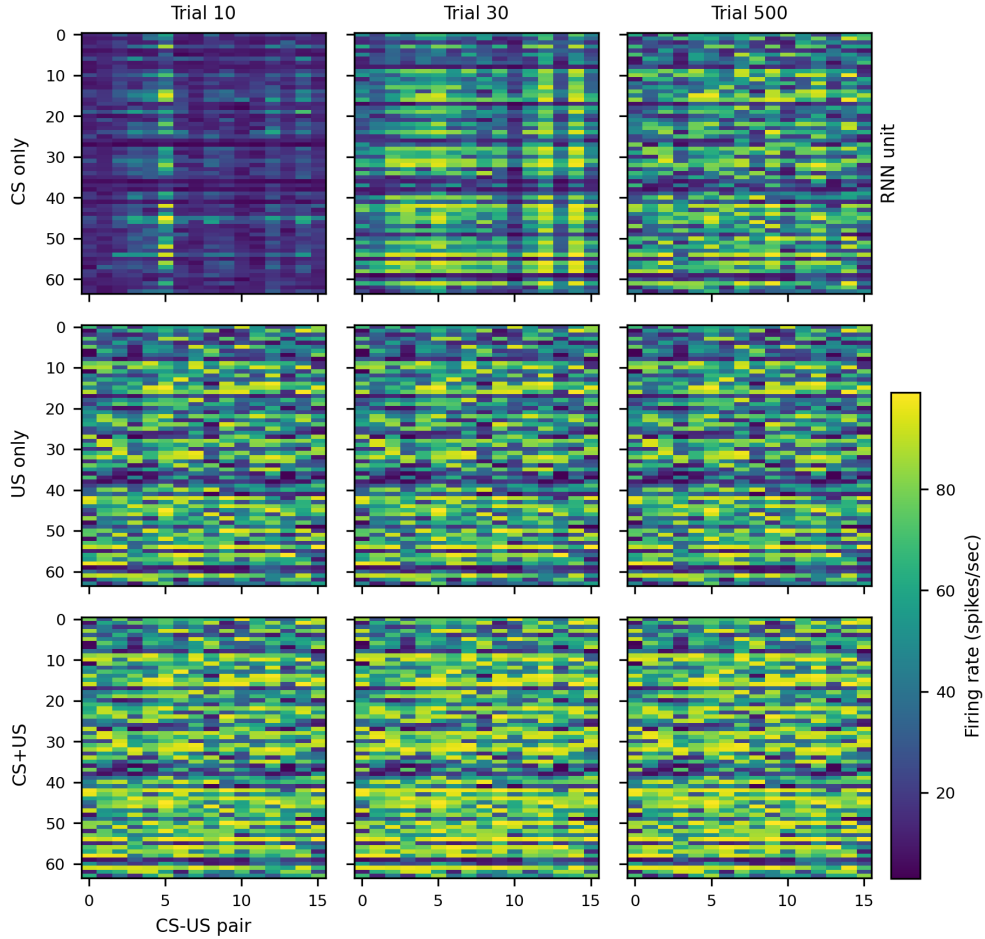
Figure S1: **RNN activity during learning**. Firing rates in response to each stimulus pair at different stages of learning. Top row shows activity in response only to the associated *CS*. Middle row shows activity in response only to the associated US. Bottom row shows activity in response to the presentation of both. Activity is measured off-line (i.e., between learning trials).

the dendritic compartment, resulting in potential mismatches between $f(V_i^{\mathrm{s}})$ and $f(p' V_i^{\mathrm{d}})$. If the learning rate η were constant across training, these mismatches would result in slow unlearning when nothing behaviorally significant is happening. In contrast, when the learning rate is gated by surprise, the learning rate $\eta = 0$ most of the times, and any mismatch between when $f(V_i^{\mathrm{s}})$ and $f(p'V_i^{\mathrm{d}})$ does not result in unlearning.

Finally consider the presynaptic potential P_j. This term is present in most learning rules and reflects the old Hebbian dictum that "neurons that fire together wire together". In particular, other things being equal, the weights of more active synapse are updated more since they have a potentially stronger influence on the postsynaptic firing rate.

We emphasize again that the fact that associative neurons are two-compartment neurons is important for the biological plausibility of the model. The gradient like term $\left[f(V_i^{\mathrm{s}}) - f(p' V_i^{\mathrm{d}}) \right]$ depends only on information available at the synapse, since it is based only on variables associated with that neuron. By definition, the presynaptic potential P_j is also available at the synapse. Finally, the learning rate is implemented by neuromodulators that are diffused to the synapses
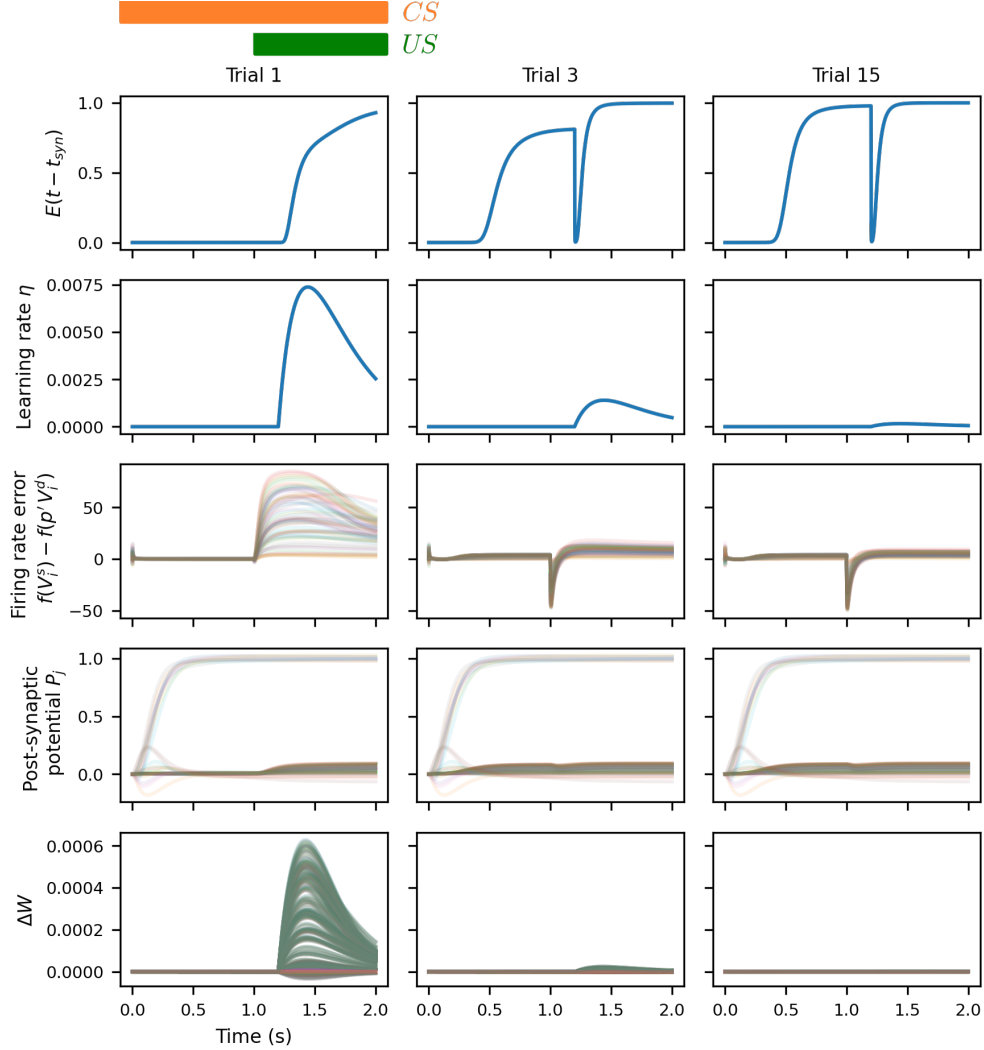
Figure S2: **Within trial dynamics of model components**. Each panel depicts the dynamics of a model component within a training trial. Columns denote the level of training. Rows denote model variables. $f(V_i^s)$ is the firing rate of associative neuron i, which is determined by its somatic voltage V_i^s. $f(p'V_i^d)$ is the (approximate) counterfactual firing rate of the neuron when only the CS is presented. E is the expectation signal for the US shown in the trial. $\eta(S)$ is the surprise-modulated learning rate. P_j is the presynaptic potentials of input neuron j. ΔW is the incremental weight change for elements of each element in W_{rnn} and W_{cs}.

of the associative network. As a result, all of the variables required to implement the learning rule are locally available at each synapse.

Three-factor Hebbian learning fails at stimulus substitution

The results in the main text have shown that our model accounts for many common patterns in classical conditioning when the RNN is trained with the predictive learning rule in equation 9. A key feature of this rule is that learning is guided by a comparison of activity in the dendritic and somatic compartments of the associative neurons.
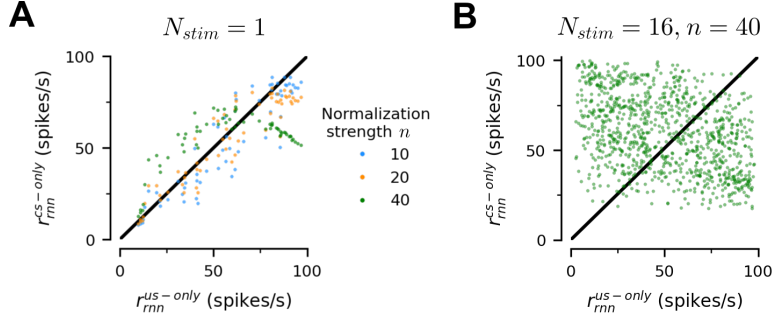
Figure S3: **Delay conditioning with Oja's rule**. Each point compares the firing rate of an associative neuron at that stage of learning for a specific *CS-US* pair when only the *US*, or only the associated *CS* are presented. Model is trained using Oja's rule. (A) Model learns stimulus substitution for different normalization strengths when $N_{\text{stim}} = 1$. Model trained for 100 trials with $\eta_0 = 2 * 10^{-4}$. (B) Models fails to learn after 1000 training trials (64 per *CS-US* pair) when $N_{\text{stim}} = 16$. For this experiment, we use $\eta_0 = 10^{-3}$.

In this section we investigate the influence of the learning rule by asking whether the same network trained using previously proposed Hebbian plasticity rules is able to account for the same phenomena. To do this, we keep all of the model components unchanged except for the learning rule. We train the model with two widely used Hebbian-like plasticity rules, Oja's rule [17] and the BCM rule [18]. We find that the resulting network either cannot learn multiple associations, or requires task specific parameter tuning.

Consider Oja's learning rule first. In this case the synaptic weights from input neuron j to associative neuron i are updated using the following rule:

$$\Delta W_{ij} = \eta(S)f(V_i^s)\left[P_j - nW_{ij}f(V_i^s)\right] \tag{31}$$

where n is the normalization strength. The normalization component is crucial, because otherwise learning would diverge. Normalization here focuses on the weights, and subjects the largest weights to the strongest normalization. We choose $n = 40$ for which the final responses to the *CS* span most of the output range of associative neurons in our model $(0 - 100\,\text{spikes/s})$.

Figure S3 shows the results of training the *RNN* with this learning rule in the delay conditioning task. We find that the network can learn well when there is a single *CS-US* pair, but it fails when it has to learn multiple associations. In fact, $r_{\text{rnn}}^{\text{us-only}}$ and $r_{\text{rnn}}^{\text{cs-only}}$ are anti-correlated in this case. This occurs because normalization introduces competition between incoming synapses to the same neuron [44], which in turn induces competition between the associations to be stored and leads to interference. More specifically, neurons that fire strongly for one pattern will sustain the harshest normalization in their incoming weights affecting the response to all other patterns. Fig. S4A also explores the role of the normalization coefficient and shows that its impact is minimal when learning a single association. This might be because final weight levels for active neurons are determined mostly by the firing rate $f(V_i^s)$ which is constant for the same association, and hence it serves as a modulator of the learning rate.

Now consider the BCM rule, which involves an alternative normalization strategy that, instead of focusing on the weights, sets a variable potentiation threshold for the postsynaptic firing rate.

4

The rule is given by:

$$\Delta W_{ij} = \eta(S) f(V_i^{\mathrm{s}}) \left[f(V_i^{\mathrm{s}}) - \alpha \theta_i \right] P_j \qquad (32)$$

where θ_i is a time-varying threshold, and α is a parameter that modulates the size of the threshold. A common choice is to make the threshold a function of the average recent firing rate, which we implement by making it an exponential moving average of the firing rate though the following differential equation:

$$\tau_\theta \frac{\mathrm{d}\theta_i}{\mathrm{d}t} = -\theta_i + f(V_i^{\mathrm{s}}) \qquad (33)$$

where the parameter τ_θ determines the temporal window of integration. In theory, this approach sounds promising, since if $r_{\mathrm{rnn},i}^{\mathrm{cs\text{-}only}} < r_{\mathrm{rnn},i}^{\mathrm{both}}$, then $f(V_i^{\mathrm{s}}) > \theta_i$ leading to potentiation and vice versa, with this logic converging to $r_{\mathrm{rnn},i}^{\mathrm{cs\text{-}only}} \approx r_{\mathrm{rnn},i}^{\mathrm{both}}$. However, as we show this is not enough to guarantee the performance of the BCM rule.

Figure S4 shows the results of training the *RNN* with the BCM rule and $\alpha = 1$. We find that with the same trial conditions used for our main results (as shown in fig. 2) the BCM rule generates intermediate amounts of conditioning, as it has a tendency to overshoot. Furthermore, fig. S4B shows that when we change the time at which the *US* appears conditioning becomes even worse, and that the problem persists for different values of τ_θ. Since the BCM rule has a tendency of underestimating the impact of the *CS*, we also explored a remedy that involved amplifying the threshold by setting $\alpha = 1.05$. Figure S4C shows that this can fix the problem for experiments in which $t_{us-on} = 1$ s, but as shown in fig. S4D, the performance of the network is still highly dependent on *US* timing. This is because the threshold, determined by a moving averaging filter of the firing rate, is highly dependent on trial specifics. Therefore, we conclude that the time-dependent threshold of the BCM rule introduces sensitivity to experimental details that cannot be overcome.

Overall, the need to fine-tune the parameters of the BCM rule to specific trial details is a general problem of Hebbian learning rules, stemming from the fact that they lack supervision. A similar point has been made by [37, 45]. In contrast, predictive learning does not demonstrate such sensitivity. Figure S4E shows that the network learns the task well for a variety of *US* onset times, without any explicit parameter tuning.

The results in this section showcase the importance of the predictive learning rule in this work, facilitated by the two-compartment nature of the associative neurons. The existence of two compartments, which separate *CS* inputs to the dendritic compartment from *US* inputs to the somatic compartment, makes it possible for the biologically plausible learning rule in eq. 9 to compare the two and guide learning using only information locally available at the synapse. In this learning rule, the activity of the somatic compartment serves as a supervisory signal for learning the weights of the inputs to the dendritic compartment until they are able to fully predict their activity in response to the *US*. In contrast, in this section we have shown that two canonical Hebbian rules struggle with this type of associative learning, in part because they do not have an analogous supervisory signal.
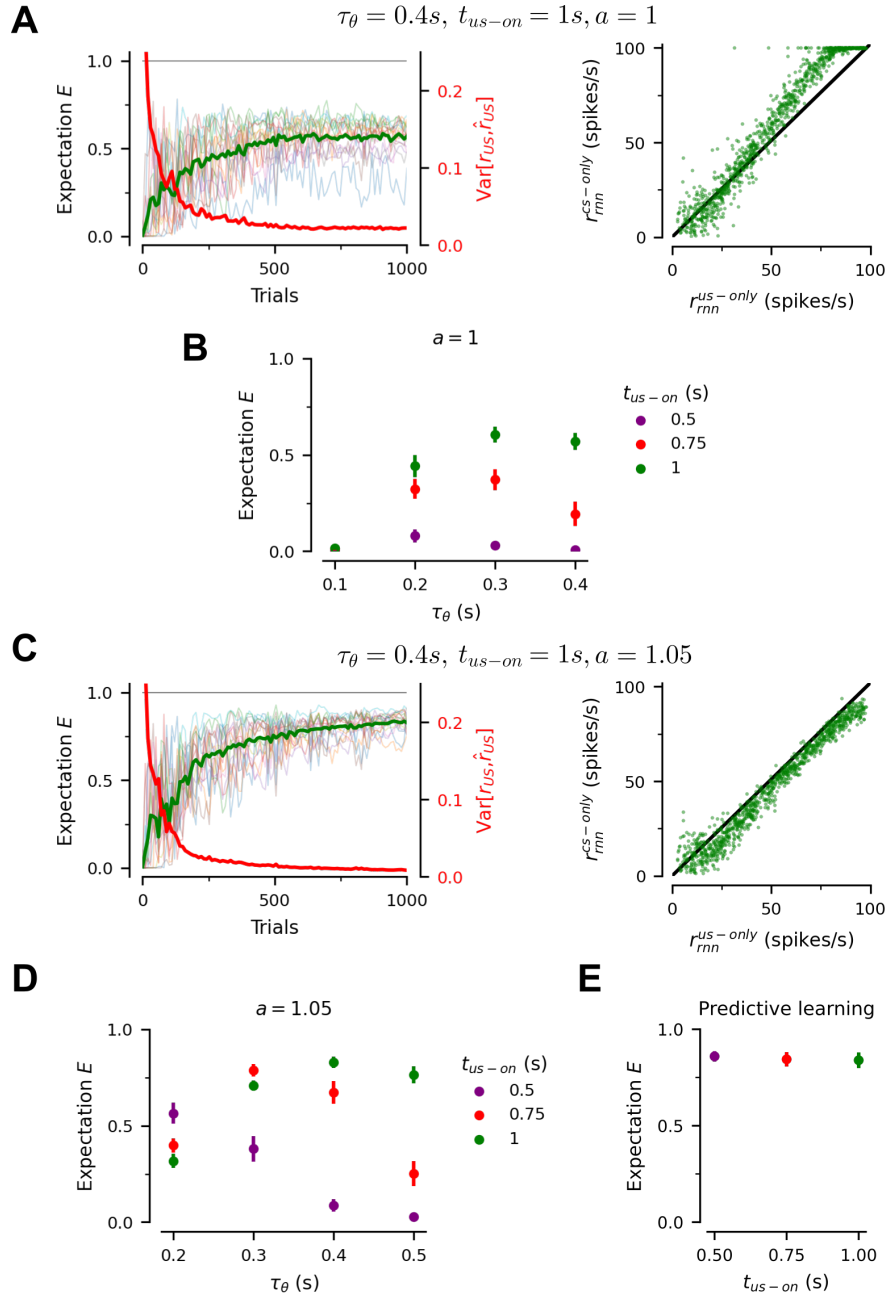
Figure S4: **Delay conditioning with BCM rule**. Model trained with $\eta_0 = 0.3$ for 1000 trials in order to learn $N_{\text{stim}} = 16$ associations. Model parameters and task conditions vary across panels. (A,C) Left: learning path. Green curve depicts the average expectation across *CS-US* pairs. Learned expectations for individual pairs are shown in faint thin lines. Right: firing rates of all associative neurons after training. (B,D) Network performance, as measured by E, as a function of the parameter τ_θ in the BCM rule and the timing at which the *US* is presented. (E) Learnt *US* expectations with our proposed predictive learning rule for different *US* timings. In contrast to the BCM rule, predictive learning is insensitive to experimental details.

Predictive coding and normative justification for the learning rule

In this section we provide further insight into the learning rule used in our model by showing that it follows directly from the objective of stimulus substitution.

Stimulus substitution states that synaptic connections change during learning so that the activity of the associative network induced by the CS ($r_{\mathrm{rnn}}^{\mathrm{cs\text{-}only}}$) becomes identical to the response induced by the US ($r_{\mathrm{rnn}}^{\mathrm{us\text{-}only}}$). It follows that the objective of stimulus substitution is to minimize the discrepancy or loss $\mathcal{L}$ between the two:

$$\mathcal{L} = \frac{1}{2}(r_{\mathrm{rnn}}^{\mathrm{cs\text{-}only}} - r_{\mathrm{rnn}}^{\mathrm{us\text{-}only}})^2 \tag{34}$$

We assume that the synaptic weights for US inputs are fixed, since these are primary reinforcers. The synaptic weights for the CS inputs are plastic, and they are shaped so that the CS elicits the same response as the US, essentially becoming predictive of the latter. Assuming a rectified linear (ReLU) activation function, $r_{\mathrm{rnn}}^{\mathrm{cs\text{-}only}}$ will obey

$$r_{\mathrm{rnn}}^{\mathrm{cs\text{-}only}} = [W^{\intercal}P]_{+} \tag{35}$$

where W are the plastic synaptic weights for the CS inputs, and P are the postsynaptic potentialsof the input CS neurons, low-pass filtered by synaptic delays.

To minimize the loss $\mathcal{L}$, we perform local gradient descent with respect to W, which leads to the following update rule:

$$\frac{\partial W}{\partial t} = -\eta \frac{\partial \mathcal{L}}{\partial W}. \tag{36}$$

This results in the following update rule between input neuron j and associative neuron i from presynaptic neuron j:

$$\Delta W_{ij} = \eta \left(r_{\mathrm{rnn},i}^{\mathrm{us\text{-}only}} - r_{\mathrm{rnn},i}^{\mathrm{cs\text{-}only}} \right) P_j. \tag{37}$$

Here, $r_{\mathrm{rnn},i}^{\mathrm{us\text{-}only}}$ acts as a "teacher" signal, in a setting that resembles self-supervised learning. Specifically, $r_{\mathrm{rnn},i}^{\mathrm{cs\text{-}only}}$ is compared to $r_{\mathrm{rnn},i}^{\mathrm{us\text{-}only}}$, and the discrepancy determines the sign and magnitude of weight change. However, only synapses from presynaptic neurons that have recently been active ($P_j > 0$) are modified. This learning rule is said to perform predictive coding, because CS inputs should predict (or anticipate) the response to the US.

An implicit requirement of the learning rule is that there has to be a way to tell apart $r_{\mathrm{rnn},i}^{\mathrm{cs\text{-}only}}$ and $r_{\mathrm{rnn},i}^{\mathrm{us\text{-}only}}$, in order to compare them. However, a neuron only has a single output at a given time. Therefore, in principle it is unclear how the two firing rates could be compared in an online fashion and within the same neuron. The 2-compartment associative neurons resolve this because the activity in the somatic compartment $f(V_i^{\mathrm{s}})$ provides a measure of $r_{\mathrm{rnn},i}^{\mathrm{us\text{-}only}}$ [1], $f(p'V_i^{\mathrm{d}})$ provides a measure of $r_{\mathrm{rnn},i}^{\mathrm{cs\text{-}only}}$, and the information available to compute the former term is available in the dendritic compartment due to backpropagating action potentials [14]. Thus, the associative neurons contain all of the information needed to implement the learning rule that yields stimulus substitution.

---

[1]In reality, as we show in eq. (16) V_i^{s} is affected by both somatic and dendritic inputs, however as we explain in the same section the influence of the dendritic inputs can never change the sign of $\left[f(V_i^{\mathrm{s}}) - f(p'\,V_i^{\mathrm{d}}) \right]$, and the resulting weight changes are always in the correct direction.

Supplementary Figures

Parameter	Value	Units	Justification
N_{stim}	16		Arbitrary, varied in text
t_{trial}	2	s	Arbitrary, varies across experiments
$t_{\mathrm{cs\text{-}off}}$	2	s	Arbitrary, varies across experiments
$t_{\mathrm{us\text{-}on}}$	1	s	Arbitrary, varies across experiments
N_{inp}	20		Arbitrary
H_{d}	8		Arbitrary, varied in text
N_{rnn}	64		Larger than number of associations learned
f_{max}	100	spikes/s	Matches plausible firing rates
β	2		For smooth change of firing rates as activation varies
$V_{1/2}$	1.5		Arbitrary
τ_{s}	100	ms	Taken from literature
τ_{l}	20	ms	Taken from literature
C	2	ms	Set by $\frac{\tau_l}{g_L}$
g_L	0.1		Chosen to be similar in range as somatic conductances from inputs
g_D	0.2		Larger than g_L to avoid large coupling attenuation and time lags
g_{inh}	3/8		Chosen to get unifrom firing rates distribution
E_{e}	14/3		Taken from [15]
E_{i}	$-1/3$		Taken from [15]
a	0.95		Arbitrary
τ_{r}	200	ms	Fit to experimental data [40]
τ_{u}	300	ms	Fit to experimental data [40]
η_0	$5 * 10^{-3}$		Chosen for fast learning when $N_{\mathrm{stim}} = 1$
Δt	1	ms	Should be 10 times smaller than smallest time constant

Table S1: Parameter value justifications. These values apply to all simulations, unless otherwise stated. Note that voltages, currents, and conductances are assumed unitless in the text; therefore capacitances have the same units as time constants.
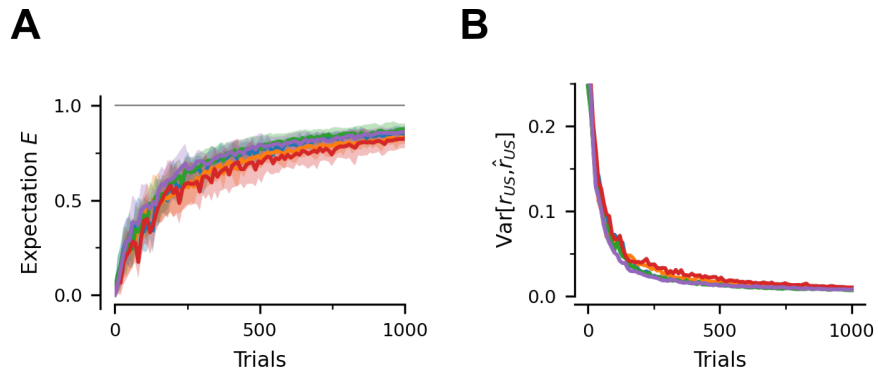
Figure S5: **Variation across training runs**. Each curve depicts a different training run. Bands represent the $\mp$ SD across stimulus pairs. (A) Expectation for each *US* after the network is presented only with the associated *CS*, averaged across all pairs at different levels of training. (B) Distance between the true representation of the *US*s (r_{us}) and their decoded representation $\hat{r}_{\mathrm{us}}$ when presented only with the associated *CS*, averaged across all pairs at different levels of training.
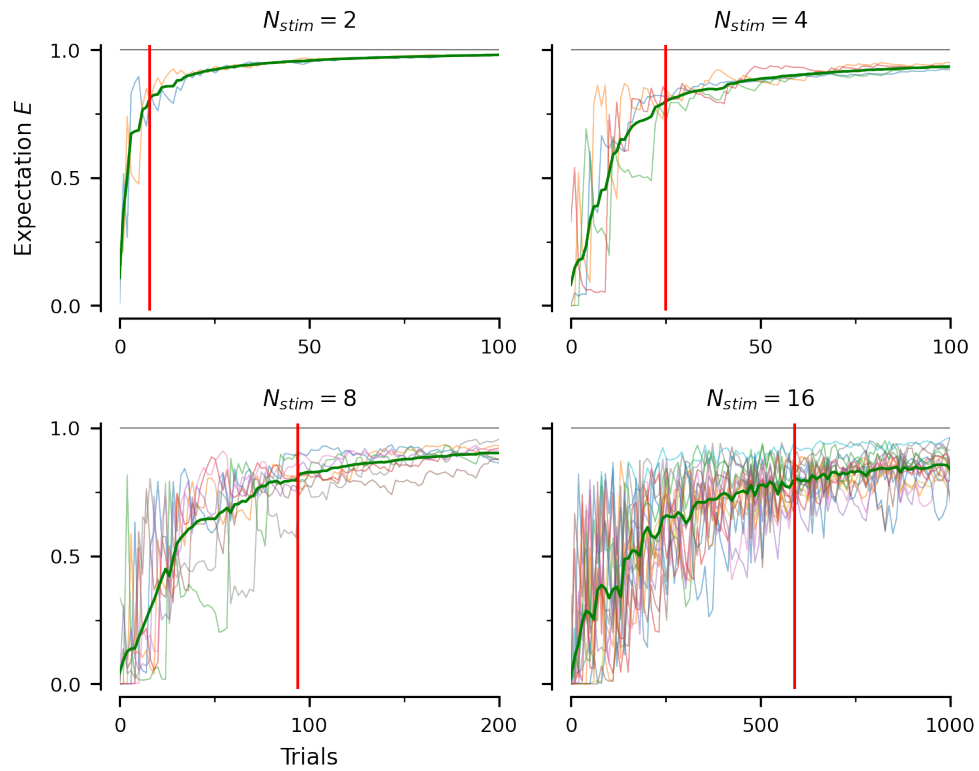
Figure S6: **Impact of the number of stimulus pairs on delay conditioning**. Learning paths for each *CS-US* pair for a single experimental run. Each thin line tracks the expectation E for a single stimulus pair. Note that the paths do not increase monotonically, which shows that there can be interference across pairs. The vertical read lines indicate the time at which the average E across pairs (thicker green line) reaches 80% performance level.
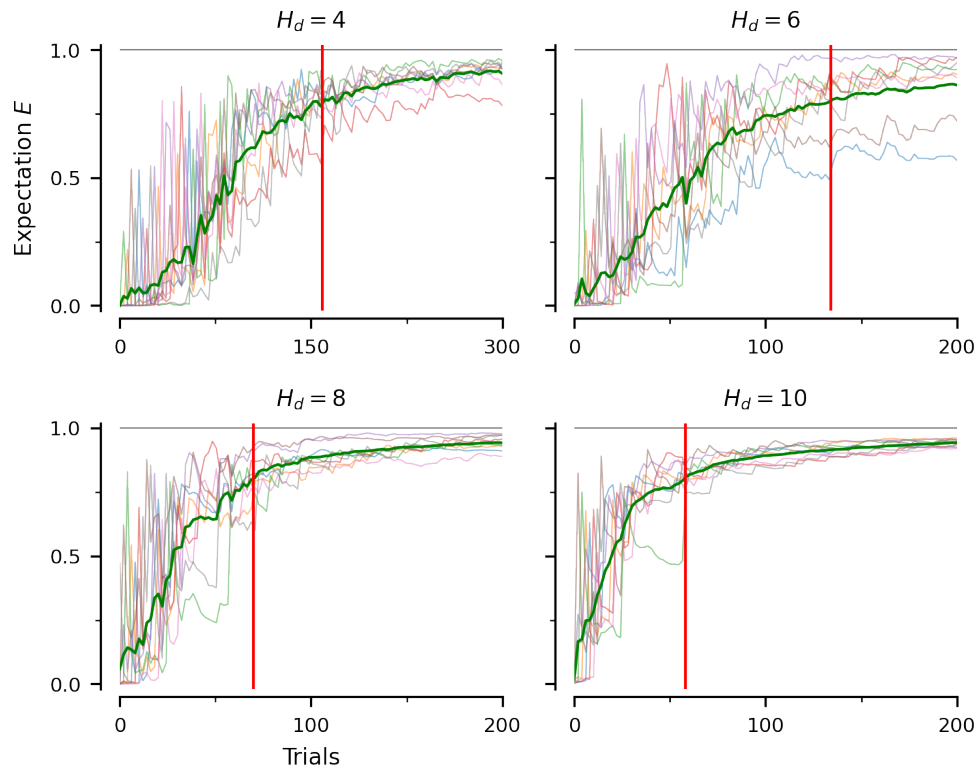
Figure S7: **Impact of the similarity on stimulus representation on delay conditioning**. Learning paths for each *CS-US* pair for a single experimental run. Each thin line tracks the expectation E for a single stimulus pair. Note that the paths do not increase monotonically, which shows that there can be interference across pairs. The vertical read lines indicate the time at which the average E across pairs (thicker green line) reaches 80% performance level.